Technische Universität Chemnitz

Sonderforschungsbereich 393

Numerische Simulation auf massiv parallelen Rechnern

Helmut Harbrecht and Reinhold Schneider

Biorthogonal wavelet bases for the boundary element method

Preprint SFB393/03-10

Preprint-Reihe des Chemnitzer SFB 393

ISSN 1619-7178 (Print) **ISSN 1619-7186** (Internet)

SFB393/03-10 **April 2003**

H. Harbrecht and R. Schneider
TU Chemnitz
Fakultät für Mathematik
D-09107 Chemnitz

http://www.tu-chemnitz.de/sfb393/

AMS Subject Classification: 47A20, 65F50, 65N38, 65R20, 65T60.

Key Words: Biorthogonal wavelet bases, norm equivalences, cancellation property, boundary integral eqautions, wavelet Galerkin schemes.

Abstract. As shown by Dahmen, Harbrecht and Schneider [7, 23, 32], the fully discrete wavelet Galerkin scheme for boundary integral equations scales linearly with the number of unknowns without compromising the accuracy of the underlying Galerkin scheme. The supposition is a wavelet basis with a sufficiently large number of vanishing moments. In this paper we present several constructions of appropriate wavelet bases on manifolds based on the biorthogonal spline wavelets of A. Cohen, I. Daubechies and J.-C. Feauveau [4]. By numerical experiments we demonstrate that it is worthwhile to spent effort on their construction to increase the performance of the wavelet Galerkin scheme considerably.

1. Introduction.

1.1. Background and Motivation.

We consider a boundary integral equation for an unknown function ρ on the closed boundary surface Γ of a domain $\Omega \in \mathbb{R}^{n+1}$

$$(\mathcal{A}\rho)(\mathbf{x}) = \int_\Gamma k(\mathbf{x},\mathbf{y})\rho(\mathbf{y})d\sigma_{\mathbf{y}} = f(\mathbf{x}), \quad \mathbf{x} \in \Gamma. \tag{1.1}$$

Herein, the boundary integral operator $\mathcal{A}$ denotes an operator of the order $2q$, that is $\mathcal{A} : H^q(\Gamma) \to H^{-q}(\Gamma)$. We assume that the kernel function $k(\mathbf{x},\mathbf{y})$ of the integral operator satisfies estimates of the type

$$\left|\partial_{\mathbf{x}}^{\boldsymbol{\alpha}}\partial_{\mathbf{y}}^{\boldsymbol{\beta}}k(\mathbf{x},\mathbf{y})\right| \le c_{\boldsymbol{\alpha},\boldsymbol{\beta}}\|\mathbf{x},\mathbf{y}\|^{-(n+2q+|\boldsymbol{\alpha}|+|\boldsymbol{\beta}|)}. \tag{1.2}$$

Examples are the single and double layer operator or the hypersingular operator with $q = -1/2, 0, +1/2$, respectively, obtained e.g. when transforming a boundary value problem for the Laplacian into an integral equation.

In general, the integral equation (1.1) is solved numerically by the boundary element method (BEM). In particular, BEM is a favourable approach for the treatment of exterior boundary value problems. One reformulates equation (1.1) as a variational problem and replaces the energy space $H^q(\Gamma)$ by finite dimensional trial spaces V_j:

$$\text{seek } \rho_j \in V_j \text{ such that} \quad (\mathcal{A}\rho_j, v_j)_{L^2(\Gamma)} = (f, v_j)_{L^2(\Gamma)} \quad \text{for all } v_j \in V_j. \tag{1.3}$$

Nevertheless, traditional discretizations suffer from a major disadvantage. The associated system matrices are densely populated. Therefore, the complexity for solving integral equations is at least $\mathcal{O}(N_J^2)$, where $N_J = \dim V_j$ denotes the number of equations. This fact restricts the maximal size of the linear equations seriously.

Modern methods for the fast solution of BEM reduce the complexity to a suboptimal rate, i.e., $\mathcal{O}(N_J \log^\alpha N_J)$, or even an optimal rate, i.e., $\mathcal{O}(N_J)$. Prominent examples for such methods are the *fast multipole method* [19], the *panel clustering* [22] or *hierarchical matrices* [21, 34].

As introduced by [1] and improved in [7, 11, 12, 13, 14, 32], the wavelet Galerkin scheme offers a further tool for the fast solution of integral equations. In fact, a Galerkin discretization by

appropriate wavelet bases results in quasi-sparse matrices. More precisely, we consider wavelets with *vanishing moments* or the *cancellation property* of order $\widetilde{d}$

$$|(v,\psi_{j,k})_{L^2(\Gamma)}| \lesssim 2^{-j(\widetilde{d}+n/2)}|v|_{W^{\widetilde{d},\infty}(\operatorname{supp}\psi_{j,\mathbf{k}})}, \tag{1.4}$$

where $|v|_{W^{\widetilde{d},\infty}(\Omega)} := \sup_{|\alpha|=\widetilde{d},\, x\in\Omega} |\partial^\alpha v(x)|$ denotes the semi-norm in $W^{\widetilde{d},\infty}(\Omega)$. Then, the kernel estimate (1.2) implies

$$|(A\psi_{j',k'},\psi_{j,k})_{L^2(\Gamma)}| \lesssim \frac{2^{-(j+j')(\widetilde{d}+n/2)}}{\operatorname{dist}(\operatorname{supp}\psi_{j,k},\operatorname{supp}\psi_{j',k'})^{n+2q+2\widetilde{d}}}.$$

As an immediate consequence of this estimate, the most matrix coefficients are negligible and can be treated as zero without deteriorating the accuracy of the underlying Galerkin scheme. Discarding these nonrelevant matrix entries is called *matrix compression*.

It has been shown in [7, 32] that only $\mathcal{O}(N_J \log^n N_J)$ significant matrix entries remain provided that the wavelet bases offer a sufficiently strong cancellation property. This means that orthonormal wavelets are not always appropriate for the solution of boundary integral equations. For matrix compression it is known that orthogonality has to be sacrificed to use higher order vanishing moments [7, 14, 32].

A strong effort has been spent on the construction of appropriate wavelet bases on surfaces [8, 16, 17, 23, 28, 32]. Our realization is based on *biorthogonal spline wavelets* derived from the multiresolution developed in [4]. These wavelets are advantageous due to several reasons. On the one hand, also a second compression step can be performed to realize a *linear* overall complexity of the wavelet Galerkin scheme, cf. [7, 32]. On the other hand, both, the primal and dual wavelets, are compactly supported which preserves the linear complexity of the fast wavelet transform also for its inverse. This is an important task for the coupling of FEM and BEM, cf. [24, 25]. Additionally, in view of the discretization of operators of positive order globally continuous wavelets are available [2, 5, 16, 23]. Moreover, the regularity of the dual wavelets is known [35], which simplifies the construction crucially.

1.2. Wavelets and Multiresolution analysis. We first focus on those aspects of biorthogonal multiresolution analyses which are useful for our purpose. Let Ω be a domain $\in \mathbb{R}^n$ or manifold $\in \mathbb{R}^{n+1}$. Then, in general, a biorthogonal multiresolution analysis consists of two nested family of finite dimensional subspaces

$$\begin{aligned} V_{j_0} \subset V_{j_0+1} \subset \cdots \subset V_j \subset V_{j+1} \cdots \subset \cdots \subset L^2(\Omega),\\ \widetilde{V}_{j_0} \subset \widetilde{V}_{j_0+1} \subset \cdots \subset \widetilde{V}_j \subset \widetilde{V}_{j+1} \cdots \subset \cdots \subset L^2(\Omega), \end{aligned} \tag{1.5}$$

such that $\dim V_j \sim \dim \widetilde{V}_j \sim 2^{nj}$ and

$$\overline{\bigcup_{j\geq j_0} V_j} = \overline{\bigcup_{j\geq j_0} \widetilde{V}_j} = L^2(\Omega). \tag{1.6}$$

The spaces $V_j = \operatorname{span}\Phi_j$, $\widetilde{V}_j = \operatorname{span}\widetilde{\Phi}_j$ are generated by biorthogonal single scale bases

$$\Phi_j = [\phi_{j,k}]_{k\in\Delta_j}, \qquad \widetilde{\Phi}_j = [\widetilde{\phi}_{j,k}]_{k\in\Delta_j}, \qquad (\Phi_j,\widetilde{\Phi}_j)_{L^2(\Omega)} = \mathbf{I},$$

where Δ_j denotes a suitable index set with cardinality $|\Delta_j| \sim 2^{nj}$. Note that here and in the sequel the basis $\Phi_j = [\phi_{j,k}]_{k\in\Delta_j}$ has to be understood as a row vector.

A final requirement is that these bases are uniformly stable, i.e., for any vector $\mathbf{c} \in l^2(\Delta_j)$ holds

$$\|\Phi_j \mathbf{c}\|_{L^2(\Omega)} \sim \|\widetilde{\Phi}_j \mathbf{c}\|_{L^2(\Omega)} \sim \|\mathbf{c}\|_{l^2(\Delta_j)} \tag{1.7}$$

uniformly in j.

If one is going to use the spaces V_j as trial spaces in (1.3) then additional properties are required. At least the primal single scale bases satisfy a locality condition

$$\operatorname{diam}\operatorname{supp}\phi_{j,k} \sim 2^{-j}.$$

Furthermore, it is assumed that the following Jackson and Bernstein type estimates hold for $s \le t \le d$, $s \le t \le \gamma$ and uniformly in j

$$\inf_{v_j\in V_j} \|u - v_j\|_{H^s(\Omega)} \lesssim 2^{j(s-t)} \|u\|_{H^t(\Omega)}, \qquad u \in H^t(\Omega), \tag{1.8}$$

and

$$\|v_j\|_{H^t(\Omega)} \lesssim 2^{j(t-s)} \|v_j\|_{H^s(\Omega)}, \qquad v_j \in V_j, \tag{1.9}$$

where $d, \gamma > 0$ are fixed constants given by

$$\begin{aligned} d &= \sup\{s \in \mathbb{R} : \inf_{v_j\in V_j} \|u - v_j\|_{L^2(\Omega)} \le 2^{-js} \|u\|_{H^s(\Omega)}\}, \\ \gamma &= \sup\{s \in \mathbb{R} : V_j \subset H^s(\Omega)\}. \end{aligned}$$

Usually, d is the maximal degree of polynomials which are locally contained in V_j and is referred to the order of exactness of the multiresolution analysis $\{V_j\}$. The parameter γ denotes the regularity or smoothness of the functions in the spaces V_j. Analogous estimates are valid for the dual multiresolution analysis $\{\widetilde{V}_j\}$ with constants $\widetilde{d}$ and $\widetilde{\gamma}$.

Instead of using only a single scale j the idea of wavelet concepts is to keep track to the increment of information between two adjacent scales j and $j+1$. The biorthogonal wavelets

$$\Psi_j = [\psi_{j,k}]_{k\in\nabla_j}, \qquad \widetilde{\Psi}_j = [\widetilde{\psi}_{j,k}]_{k\in\nabla_j}, \qquad (\Psi_j, \widetilde{\Psi}_j)_{L^2(\Omega)} = \mathbf{I},$$

where $\nabla_j = \Delta_{j+1} \setminus \Delta_j$ are the bases of *uniquely* determined complement spaces $W_j = \operatorname{span}\Psi_j$, $\widetilde{W}_j = \operatorname{span}\widetilde{\Psi}_j$ satisfying

$$\begin{aligned} V_{j+1} &= V_j \oplus W_j, \qquad V_j \cap W_j = \{0\}, \qquad W_j \perp \widetilde{V}_j, \\ \widetilde{V}_{j+1} &= \widetilde{V}_j \oplus \widetilde{W}_j, \qquad \widetilde{V}_j \cap \widetilde{W}_j = \{0\}, \qquad \widetilde{W}_j \perp V_j. \end{aligned} \tag{1.10}$$

We claim that the primal wavelets $\psi_{j,k}$ are also local with respect to the corresponding scale j, i.e.

$$\operatorname{diam}\operatorname{supp}\psi_{j,k} \sim 2^{-j}, \tag{1.11}$$

and we will normalize the wavelets such that $\|\psi_{j,k}\|_{L_2(\Omega)} \sim \|\widetilde{\psi}_{j,k}\|_{L_2(\Omega)} \sim 1$. Furthermore, we suppose that the wavelet bases

$$\Psi = [\Psi_j]_{j\ge j_0-1}, \qquad \widetilde{\Psi} = [\widetilde{\Psi}_j]_{j\ge j_0-1}, \tag{1.12}$$

($\Psi_{j_0-1} := \Phi_{j_0}$, $\widetilde{\Psi}_{j_0-1} := \widetilde{\Phi}_{j_0}$), are Riesz bases of $L_2(\Omega)$.

The assumptions that (1.8) and (1.9) hold with some constants γ and $\widetilde{\gamma}$ relative to $\{V_j\}$, $\{\widetilde{V}_j\}$ provide a convenient device for switching between the norms $\|\cdot\|_{H^t(\Omega)}$ and corresponding sums of weighted wavelet coefficients. Namely, the following norm equivalences hold

$$\begin{aligned} \|v\|^2_{H^s(\Omega)} &\sim \sum_{j\geq j_0-1}\sum_{k\in\nabla_j} 2^{js}|(v,\widetilde{\psi}_{j,k})_{L^2(\Omega)}|^2, \qquad s\in(-\widetilde{\gamma},\gamma), \\ \|v\|^2_{H^s(\Omega)} &\sim \sum_{j\geq j_0-1}\sum_{k\in\nabla_j} 2^{js}|(v,\psi_{j,k})_{L^2(\Omega)}|^2, \qquad s\in(-\gamma,\widetilde{\gamma}), \end{aligned} \tag{1.13}$$

see e.g. [6, 32] for the details. Note that for $s = 0$ the norm equivalence implies the Riesz property of the wavelet bases.

From (1.10) we deduce that the primal wavelets provide the cancellation property (1.4) of order $\widetilde{d}$. Moreover, the cancellation property holds also with respect to the dual wavelets with the parameter d.

To end this section, we mention that linear complexity of the wavelet Galerkin scheme is realized when using wavelets fulfilling the relation

$$d < \widetilde{d} + 2q, \tag{1.14}$$

where $2q$ denotes the order of the boundary integral operator, cf. [7, 23, 32]. Moreover, if

$$\widetilde{\gamma} > -q/2, \tag{1.15}$$

the main diagonal of the system matrix defines a simple preconditioning for ths linear system of equations arising boundary integral operators of nonzero order [6, 9, 32].

1.3. Refinement Relations and Stable Completions. For the construction of multiresolution bases we are interested in the *filter coefficients* or *mask coefficients* associated with the scaling functions and the wavelets. Since boundary functions have to be introduced, these filter coefficients are not fixed like in the stationary case. Therefore, we compute the full *two scale relations*

$$\begin{aligned} \Phi_j &= \Phi_{j+1}\mathbf{M}_{j,0}, \qquad \Psi_j = \Phi_{j+1}\mathbf{M}_{j,1}, \\ \widetilde{\Phi}_j &= \widetilde{\Phi}_{j+1}\widetilde{\mathbf{M}}_{j,0}, \qquad \widetilde{\Psi}_j = \widetilde{\Phi}_{j+1}\widetilde{\mathbf{M}}_{j,1}, \end{aligned} \tag{1.16}$$

where $\mathbf{M}_{j,0}, \widetilde{\mathbf{M}}_{j,0} \in \mathbb{R}^{|\Delta_{j+1}|\times|\Delta_j|}$ and $\mathbf{M}_{j,0}, \widetilde{\mathbf{M}}_{j,0} \in \mathbb{R}^{|\Delta_{j+1}|\times|\nabla_j|}$. Note that these matrices will be banded and only the filter coefficients for some specific scaling functions and wavelets have to be modified. That way, the advantages of the stationary and shift-invariant case are preserved as far as possible.

In the sequel, our proceeding is the following. We first construct biorthogonal single scale bases in refinable spaces V_j and $\widetilde{V}_j$. The parameters $d, \widetilde{d}, \gamma$ and $\widetilde{\gamma}$ are constituted by these single scale bases. According to (1.10) the complementary spaces W_j and $\widetilde{W}_j$ are determined uniquely. But the biorthogonal wavelet bases generating these complementary spaces are not determined uniquely. Each pair of matrices $\mathbf{M}_{j,1}, \widetilde{\mathbf{M}}_{j,1}$ satisfying

$$[\mathbf{M}_{j,0}, \mathbf{M}_{j,1}]^T[\widetilde{\mathbf{M}}_{j,0}, \widetilde{\mathbf{M}}_{j,1}] = \mathbf{I}$$

defines wavelets (especially Riesz bases in $L^2(\Omega)$) via their two scale relations (1.16). But, for instance, this straightforward construction does not imply fixed and finite masks for the wavelets. Hence, in order to define suitable wavelet bases we utilize the concept of the *stable completion* [3]. This concept is universal and often employed in the sequel.

DEFINITION 1.1. *Let $\breve{\Psi}_j = [\breve{\psi}_{j,k}]_{k\in\nabla_j} \subset V_{j+1}$ be a given collection of functions satisfying*

$$\breve{\Psi}_j = \Phi_{j+1}\breve{\mathbf{M}}_{j,1}, \qquad \breve{\mathbf{M}}_{j,1} \in \mathbb{R}^{|\Delta_{j+1}|\times|\nabla_j|},$$

such that $[\mathbf{M}_{j,0}, \breve{\mathbf{M}}_{j,1}]$ is invertible. We define the matrix $[\mathbf{G}_{j,0}, \mathbf{G}_{j,1}]$ with $\mathbf{G}_{j,0} \in \mathbb{R}^{|\Delta_{j+1}|\times|\Delta_j|}$ and $\mathbf{G}_{j,1} \in \mathbb{R}^{|\Delta_{j+1}|\times|\nabla_j|}$ as the inverse of $[\mathbf{M}_{j,0}, \breve{\mathbf{M}}_{j,1}]^T$, i.e.

$$[\mathbf{M}_{j,0}, \breve{\mathbf{M}}_{j,1}]^T[\mathbf{G}_{j,0}, \mathbf{G}_{j,1}] = \mathbf{I}. \tag{1.17}$$

The collection $\breve{\Psi}_j$ is called a stable completion of Φ_j if

$$\left\|[\mathbf{M}_{j,0}, \breve{\mathbf{M}}_{j,1}]_{l^2(\Delta_{j+1})}\right\| \sim \|[\mathbf{G}_{j,0}, \mathbf{G}_{j,1}]\|_{l^2(\Delta_{j+1})} \sim 1. \tag{1.18}$$

We derive the desired wavelet basis by projecting the stable completion onto W_j, cf. [10]. In terms of the refinement matrices, the matrix $\mathbf{M}_{j,1}$ is defined by

$$\mathbf{M}_{j,1} = \left[\mathbf{I} - \mathbf{M}_{j,0}\big(\widetilde{\mathbf{M}}_{j,0}\big)^T\right]\breve{\mathbf{M}}_{j,1} =: \breve{\mathbf{M}}_{j,1} - \mathbf{M}_{j,0}\mathbf{L}_j. \tag{1.19}$$

One readily verifies that the matrix $\mathbf{L}_j \in \mathbb{R}^{|\Delta_j|\times|\nabla_j|}$ satisfies

$$\mathbf{L}_j = \big(\widetilde{\mathbf{M}}_{j,0}\big)^T\breve{\mathbf{M}}_{j,1} = \big(\widetilde{\Phi}_j, \breve{\Psi}_j\big)_{L^2(\Omega)}. \tag{1.20}$$

Moreover, one concludes from the identity

$$\mathbf{I} = [\mathbf{M}_{j,0}, \mathbf{M}_{j,1}]^T[\widetilde{\mathbf{M}}_{j,0}, \widetilde{\mathbf{M}}_{j,1}] = \begin{bmatrix}\mathbf{I} & -\mathbf{L}_j\\ \mathbf{0} & \mathbf{I}\end{bmatrix}^T [\mathbf{M}_{j,0}, \breve{\mathbf{M}}_{j,1}]^T[\mathbf{G}_{j,0}, \mathbf{G}_{j,1}] \begin{bmatrix}\mathbf{I} & \mathbf{0}\\ \big(\mathbf{L}_j\big)^T & \mathbf{I}\end{bmatrix}$$

the equality

$$[\widetilde{\mathbf{M}}_{j,0}, \widetilde{\mathbf{M}}_{j,1}] = [\mathbf{G}_{j,0} + \mathbf{G}_{j,1}\big(\mathbf{L}_j\big)^T, \mathbf{G}_{j,1}],$$

i.e. $\widetilde{\mathbf{M}}_{j,1} = \mathbf{G}_{j,1}$. Note that a compactly supported stable completion implies compactly supported wavelet bases.

REMARK 1.2. *The definition of $\mathbf{M}_{j,1}$ implies*

$$\Psi_j = \Phi_{j+1}\mathbf{M}_{j,1} = \Phi_{j+1}\breve{\mathbf{M}}_{j,1} - \Phi_{j+1}\breve{\mathbf{M}}_{j,0}\mathbf{L}_j = \breve{\Psi}_j - \Phi_j\mathbf{L}_j.$$

Consequently, similarly to [33], the wavelets Ψ_j are obtained by updating $\breve{\Psi}_j$ by linear combinations of the coarse level generators Φ_j.

2. Construction of Wavelets on Manifolds.

2.1. Biorthogonal Spline Multiresolution on the Interval. Our approach is based on the biorthogonal spline multiresolution on $\mathbb{R}$ developed by A. Cohen, I. Daubechies and J.-C. Feauveau [4]. These functions have several properties which make them favourite candidates for the wavelet Galerkin scheme.

– The primal multiresolution consists of cardinal B-splines of the order d as scaling functions. Therefore, we have to deal only with piecewise polynomials. This simplifies the construction of wavelet bases on manifolds and the computation of the matrix coefficients in the Galerkin matrix. We like to point out that the primal multiresolution realizes the order of approximation d. The regularity of these ansatz functions is $\gamma^{\mathbb{R}} = d - 1/2$.

– The dual multiresolution is generated by compactly supported scaling functions realizing the order of approximation $\widetilde{d} \in \mathbb{N}$ ($d + \widetilde{d}$ even). According to [35] their regularity $\widetilde{\gamma}^{\mathbb{R}}$ is known.

According to [10], based on these scaling functions, we can construct refinable spaces $V_j^{[0,1]}$, $\widetilde{V}_j^{[0,1]}$ which contain all polynomials of degree less than d, $\widetilde{d}$, respectively, Clearly, the goal is to construct a wavelet basis such that only a few boundary wavelets do not coincide with translates and dilates of the Cohen-Daubechies-Feauveau wavelets [4]. For the treatment of boundary integral equations we focus mainly on piecewise constant and linear wavelets, i.e., $d = 1$ and $d = 2$. On the level j, we consider the interval $[0, 1]$ subdivided into 2^j equidistant subintervals. Then, of course, $V_j^{[0,1]}$ is the space generated by 2^j and $2^j + 1$ piecewise constant and linear scaling functions, respectively. We prefer the Haar basis and the hierarchical basis on the given partition to define suitable stable completions. In fact, utilizing these stable completions the interior wavelets coincide with the Cohen-Daubechies-Feauveau wavelets, cf. [23]. Unfortunately, the general situation is not that simple since we have to modify the boundary functions. We refer to [10, 23] for the details.

According to [10] the following statements hold.

– The collections $\Psi^{[0,1]}$ and $\widetilde{\Psi}^{[0,1]}$ given by (1.12) define biorthogonal Riesz bases in $L^2([0, 1])$.

– The functions of $\Psi^{[0,1]}$ and $\widetilde{\Psi}^{[0,1]}$ have $\widetilde{d}$ and d vanishing moments, respectively.

– The functions of the collections $\Psi^{[0,1]}$ and $\widetilde{\Psi}^{[0,1]}$ have the same regularity as the biorthogonal spline wavelets in $L^2(\mathbb{R})$ [35]. Therefore, the norm equivalences (1.13) are valid for $\gamma = \gamma^{\mathbb{R}} = d-1/2$ and $\gamma = \widetilde{\gamma}^{\mathbb{R}}$.

In view of operators of positive order, e.g. the hypersingular operator, we need globally continuous wavelet bases. According to [16, 23], for their construction, the primal and dual scaling functions as well as the stable completion are required to satisfy the following boundary conditions.

– Only one function each of the collections $\Phi_j^{[0,1]}$ and $\widetilde{\Phi}_j^{[0,1]}$, respectively, is nonvanishing at the interval endpoints $x = 0$ and $x = 1$. that is

$$\phi_{j,k}^{[0,1]}(0) = \begin{cases} 2^{j/2}, & k = 0, \\ 0, & k \neq 0, \end{cases} \qquad \widetilde{\phi}_{j,k}^{[0,1]}(0) = \begin{cases} 2^{j/2}c, & k = 0, \\ 0, & k \neq 0, \end{cases} \tag{2.1}$$

$c \neq 0$, and likewise for $x = 1$ and $k = |\triangle_j^{[0,1]}|$.

– The stable completion $\breve{\Psi}_j^{[0,1]}$ fulfills zero boundary conditions

$$\breve{\psi}_{j,k}^{[0,1]}(0) = \breve{\psi}_{j,k}^{[0,1]}(1) = 0, \qquad k \in \nabla_j^{[0,1]}. \tag{2.2}$$

Moreover, the symmetry condition

$$\breve{\psi}_{j,k}^{[0,1]}(x) = \breve{\psi}_{j,|\nabla_j^{[0,1]}|-k}^{[0,1]}(1-x) \tag{2.3}$$

holds for all $k \in \nabla_j^{[0,1]}$.

Note that the first condition can be realized by a suitable change of bases, cf. [16, 23]. The construction of stable completions satisfying the second condition is addressed in [10, 16, 23]. Note that in the case of the piecewise linears, the hierarchical basis satisfies (2.2) and (2.3).

2.2. Wavelets on the Unit Square. In general, it suffices to consider two dimensional wavelets for the treatment of boundary integral equations. Hence, we restrict ourselves to the two dimensional case since the construction keeps simple. For the higher dimensional case we refer to [16, 23].

2.2.1. Biorthogonal Scaling Functions. The canonical definition of biorthogonal multiresolutions on the unit square $\square := [0,1]^2$ is to take tensor products of the univariate constructions. That is, the collections of scaling functions are given by

$$\Phi_j^{\square} = \Phi_j^{[0,1]} \otimes \Phi_j^{[0,1]}, \qquad \widetilde{\Phi}_j^{\square} = \widetilde{\Phi}_j^{[0,1]} \otimes \widetilde{\Phi}_j^{[0,1]}, \tag{2.4}$$

with the index set $\Delta_j^{\square} = \Delta_j^{[0,1]} \times \Delta_j^{[0,1]}$. Consequently, the associated refinement matrices are

$$\mathbf{M}_{j,0}^{\square} = \mathbf{M}_{j,0}^{[0,1]} \otimes \mathbf{M}_{j,0}^{[0,1]}, \qquad \widetilde{\mathbf{M}}_{j,0}^{\square} = \widetilde{\mathbf{M}}_{j,0}^{[0,1]} \otimes \widetilde{\mathbf{M}}_{j,0}^{[0,1]}. \tag{2.5}$$

As an immediate consequence of the univariate case, the spaces $V_j^{\square} := \operatorname{span} \Phi_j^{\square}$ and $\widetilde{V}_j^{\square} := \operatorname{span} \widetilde{\Phi}_j^{\square}$ are nested and dense in $L^2(\square)$. Clearly, these spaces are exact of the order d and $\widetilde{d}$, respectively. We emphasize that the complement spaces $W_j^{\square}$ and $\widetilde{W}_j^{\square}$ are uniquely determined by (1.10). With this in mind, the remainder of this subsection is dedicated to the construction of biorthogonal wavelet bases $\Psi_j^{\square}$ and $\widetilde{\Psi_j^{\square}}$ with $W_j^{\square} := \operatorname{span} \Psi_j^{\square}$ and $\widetilde{W}_j^{\square} := \operatorname{span} \widetilde{\Psi}_j^{\square}$.

2.2.2. Tensor Product Wavelets. First, we introduce the simplest construction, namely tensor product wavelets

$$\Psi_j^{\square} = \big[\Phi_j^{[0,1]} \otimes \Psi_j^{[0,1]}, \Psi_j^{[0,1]} \otimes \Phi_j^{[0,1]}, \Psi_j^{[0,1]} \otimes \Psi_j^{[0,1]}\big].$$

Then, the refinement matrices are defined via

$$\mathbf{M}_{j,1}^{\square} = \begin{bmatrix} \mathbf{M}_{j,0}^{[0,1]} \otimes \mathbf{M}_{j,1}^{[0,1]} \\ \mathbf{M}_{j,1}^{[0,1]} \otimes \mathbf{M}_{j,0}^{[0,1]} \\ \mathbf{M}_{j,1}^{[0,1]} \otimes \mathbf{M}_{j,1}^{[0,1]} \end{bmatrix}, \qquad \widetilde{\mathbf{M}}_{j,1}^{\square} = \begin{bmatrix} \widetilde{\mathbf{M}}_{j,0}^{[0,1]} \otimes \widetilde{\mathbf{M}}_{j,1}^{[0,1]} \\ \widetilde{\mathbf{M}}_{j,1}^{[0,1]} \otimes \widetilde{\mathbf{M}}_{j,0}^{[0,1]} \\ \widetilde{\mathbf{M}}_{j,1}^{[0,1]} \otimes \widetilde{\mathbf{M}}_{j,1}^{[0,1]} \end{bmatrix}.$$

Hence, we differ three types of wavelets on $\square$, cf. Figures 2.1 and 2.2. The first type is the tensor product $\phi_{j,k}^{[0,1]} \otimes \psi_{j,l}^{[0,1]}$. The second type is the tensor product of $\psi_{j,k}^{[0,1]} \otimes \phi_{j,l}^{[0,1]}$. The third type consists of the tensor product of two wavelets $\psi_{j,k}^{[0,1]} \otimes \phi_{j,l}^{[0,1]}$. We mention that $|\Delta_j^{[0,1]}| \approx |\nabla_j^{[0,1]}|$ implies nearly identical cardinalities of the three types of wavelets.

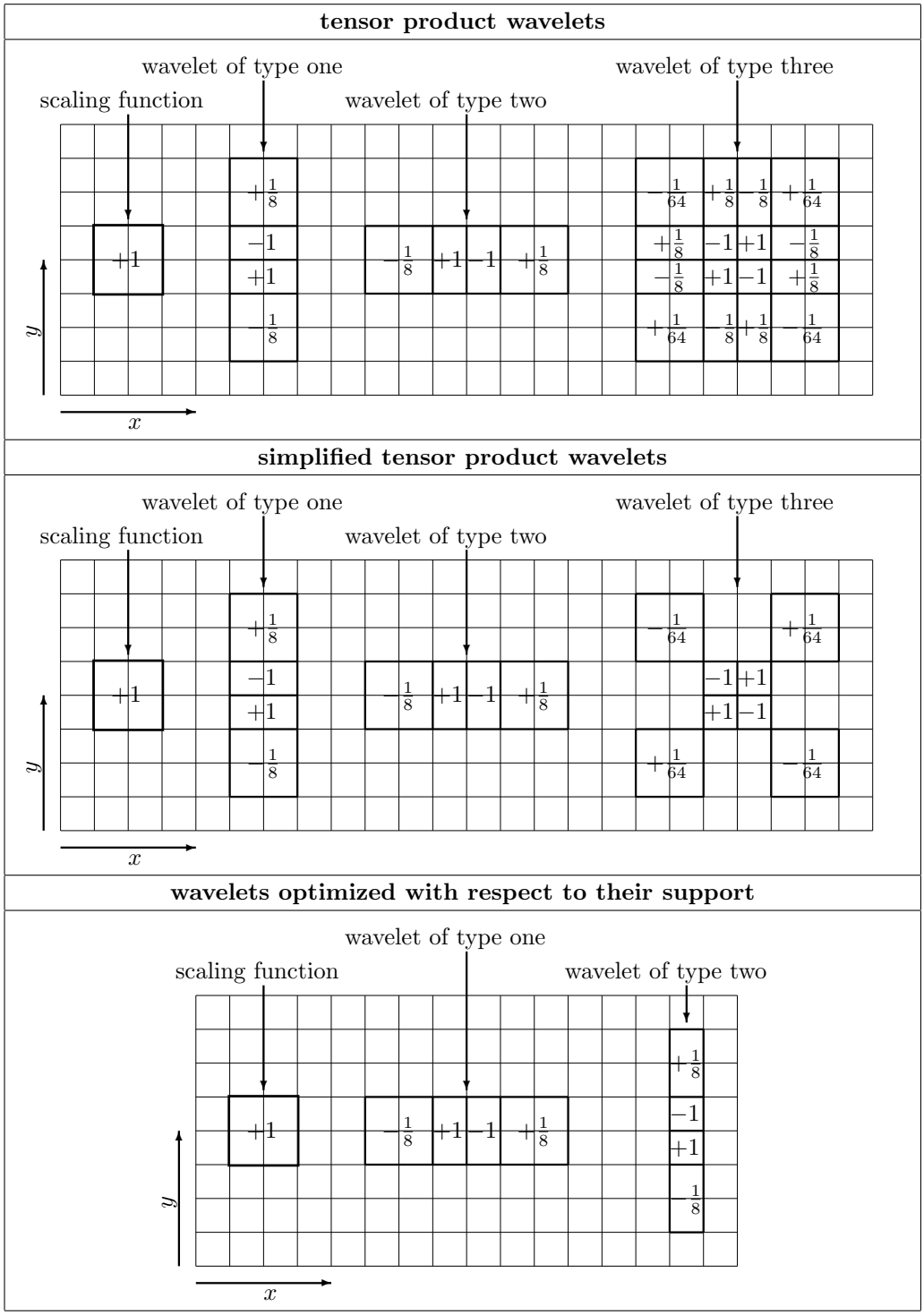

FIG. 2.1. *Interior piecewise constant wavelets with three vanishing moments. The boundary wavelets are not plotted.*

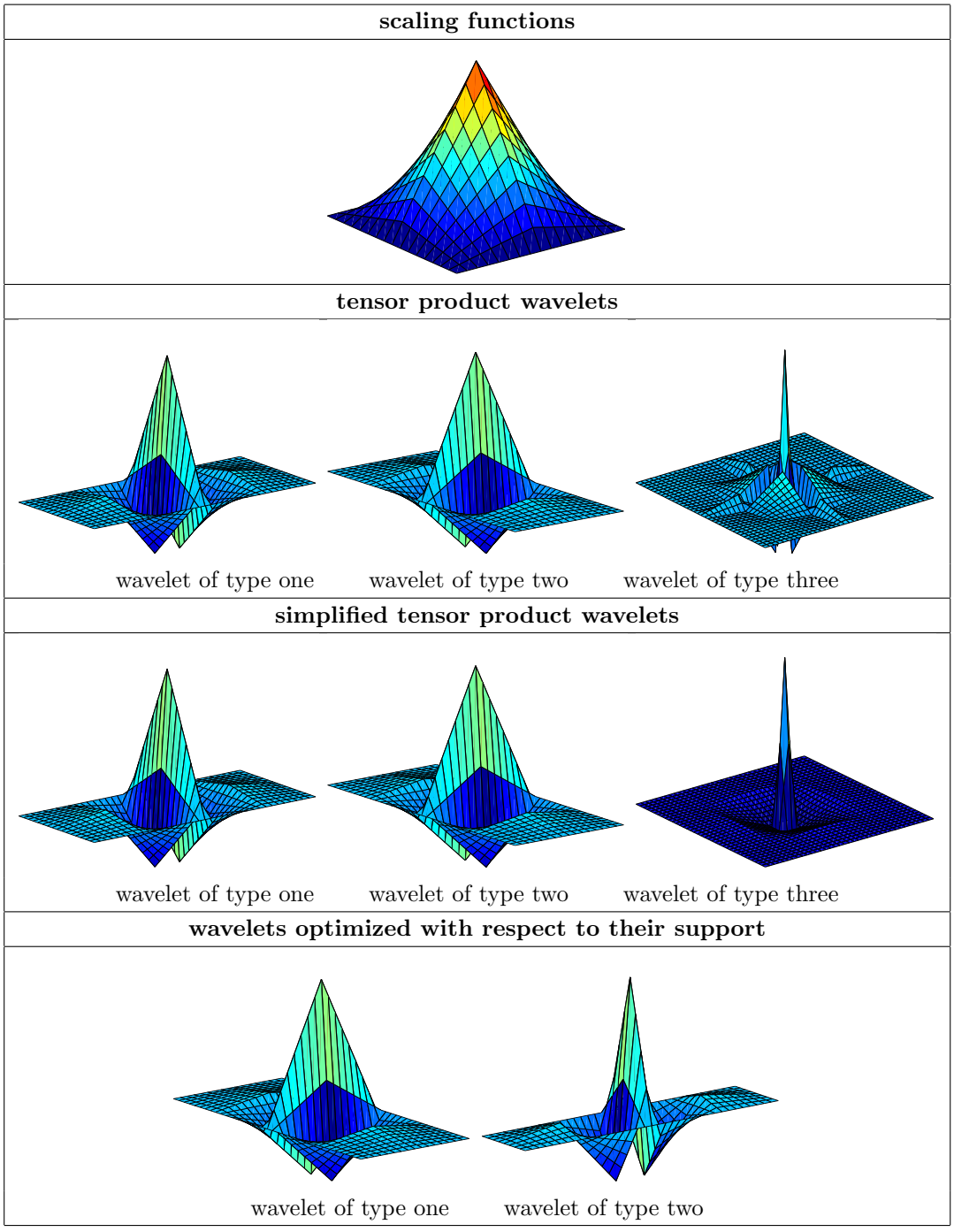

FIG. 2.2. *Interior piecewise linear wavelets with four vanishing moments. The boundary wavelets are not plotted.*

2.2.3. Simplified Tensor Product Wavelets. We consider an extension of the tensor product construction. As we will see it replaces the the third type wavelets by smoother ones. We mention that this simplifies numerical integration, for instance in the Galerkin scheme.

The idea is to involve a suitable stable completion on the unit square. Based on the univariate case

it can be defined by the collection

$$\breve{\Psi}_j^{\square} = \big[\Phi_j^{[0,1]} \otimes \breve{\Psi}_j^{[0,1]}, \breve{\Psi}_j^{[0,1]} \otimes \Phi_j^{[0,1]}, \breve{\Psi}_j^{[0,1]} \otimes \breve{\Psi}_j^{[0,1]}\big].$$

The refinement matrices $\breve{\mathbf{M}}_{j,1}^{\square}$, $\mathbf{G}_{j,0}^{\square}$ and $\mathbf{G}_{j,1}^{\square}$ are computed by

$$\breve{\mathbf{M}}_{j,1}^{\square} = \begin{bmatrix} \mathbf{M}_{j,0}^{[0,1]} \otimes \breve{\mathbf{M}}_{j,1}^{[0,1]} \\ \breve{\mathbf{M}}_{j,1}^{[0,1]} \otimes \mathbf{M}_{j,0}^{[0,1]} \\ \breve{\mathbf{M}}_{j,1}^{[0,1]} \otimes \breve{\mathbf{M}}_{j,1}^{[0,1]} \end{bmatrix}, \qquad \mathbf{G}_{j,0}^{\square} = \mathbf{G}_{j,0}^{[0,1]} \otimes \mathbf{G}_{j,0}^{[0,1]}, \qquad \mathbf{G}_{j,1}^{\square} = \begin{bmatrix} \mathbf{G}_{j,0}^{[0,1]} \otimes \mathbf{G}_{j,1}^{[0,1]} \\ \mathbf{G}_{j,1}^{[0,1]} \otimes \mathbf{G}_{j,0}^{[0,1]} \\ \mathbf{G}_{j,1}^{[0,1]} \otimes \mathbf{G}_{j,1}^{[0,1]} \end{bmatrix}.$$

As one readily verifies, the matrix $\mathbf{L}_j^{\square}$ is given by

$$\mathbf{L}_j^{\square} = \begin{bmatrix} \mathbf{I}^{(|\Delta_j^{[0,1]}|)} \otimes \mathbf{L}_j^{[0,1]} \\ \mathbf{L}_j^{[0,1]} \otimes \mathbf{I}^{(|\Delta_j^{[0,1]}|)} \\ \mathbf{L}_j^{[0,1]} \otimes \mathbf{L}_j^{[0,1]} \end{bmatrix}.$$

This implies

$$\mathbf{M}_{j,1}^{\square} = \breve{\mathbf{M}}_{j,1}^{\square} - \mathbf{M}_{j,0}^{\square}\mathbf{L}_j^{\square} = \begin{bmatrix} \mathbf{M}_{j,0}^{[0,1]} \otimes \mathbf{M}_{j,1}^{[0,1]} \\ \mathbf{M}_{j,1}^{[0,1]} \otimes \mathbf{M}_{j,0}^{[0,1]} \\ \breve{\mathbf{M}}_{j,1}^{[0,1]} \otimes \breve{\mathbf{M}}_{j,1}^{[0,1]} - \big(\mathbf{M}_{j,0}^{[0,1]} \otimes \mathbf{M}_{j,0}^{[0,1]}\big)\big(\mathbf{L}_j^{[0,1]} \otimes \mathbf{L}_j^{[0,1]}\big) \end{bmatrix}.$$

Hence, we differ again three types of wavelets on $\square$. The first and the second type coincide with the tensor product wavelets, see Figures 2.1 and 2.2. But now the third type consists of the tensor product of the stable completion $\breve{\psi}_{j,\mathbf{k}}^{\square} = \breve{\psi}_{j,k}^{[0,1]} \otimes \breve{\psi}_{j,l}^{[0,1]}$ and certain scaling functions $\phi_{j,\mathbf{k}'}^{\square} = \phi_{j,k'}^{[0,1]} \otimes \phi_{j,l'}^{[0,1]}$ of the coarse grid j. In general, the support of this wavelet does not depend on the choice of the stable completion. But choosing a stable completion on $[0,1]$ with small supports, the product $\breve{\psi}_{j,k}^{[0,1]} \otimes \breve{\psi}_{j,l}^{[0,1]} \in V_{j+1}^{\square}$ has also small support. Since the additional scaling functions belong to $V_j^{\square}$, the wavelet is smoother than the corresponding tensor product wavelet.

2.2.4. Wavelets optimized with respect to their Supports. Last, we consider a more advanced construction which yields wavelets with very small supports. We define the wavelet functions via the collections

$$\begin{aligned} \Psi_j^{\square} &= \big[\Psi_j^{[0,1]} \otimes \Phi_j^{[0,1]}, \Phi_{j+1}^{[0,1]} \otimes \Psi_j^{[0,1]}\big], \\ \widetilde{\Psi}_j^{\square} &= \big[\widetilde{\Psi}_j^{[0,1]} \otimes \widetilde{\Phi}_j^{[0,1]}, \widetilde{\Phi}_{j+1}^{[0,1]} \otimes \widetilde{\Psi}_j^{[0,1]}\big]. \end{aligned} \tag{2.6}$$

LEMMA 2.1. *The collections of wavelets $\Psi_j^{\square}$ and $\widetilde{\Psi}_j^{\square}$ introduced by* (2.6) *define biorthogonal wavelet bases with respect to the multiresolution given by $\Phi_j^{\square}$ and $\widetilde{\Phi}_j^{\square}$.*

Proof. One readily verifies the equations

$$\big(\psi_{j,\mathbf{k}}^{\square}, \widetilde{\phi}_{j,\mathbf{k}'}^{\square}\big)_{L^2(\square)} = \big(\widetilde{\psi}_{j,\mathbf{k}}^{\square}, \phi_{j,\mathbf{k}'}^{\square}\big)_{L^2(\square)} = 0, \qquad \mathbf{k} \in \nabla_j^{\square}, \quad \mathbf{k} \in \Delta_j^{\square},$$

by inserting the definition (2.6) of the wavelet functions and employing the biorthogonality on the interval. Consequently, in order to show the biorthogonality of the wavelets, we only have to prove that

$$\big(\psi_{j,\mathbf{k}}^{\square}, \widetilde{\psi}_{j,\mathbf{k}'}^{\square}\big)_{L^2(\square)} = \delta_{\mathbf{k},\mathbf{k}'}, \qquad \mathbf{k}, \mathbf{k}' \in \Delta_j^{\square}.$$

But similar to above this is also an immediate consequence of the biorthogonality on the interval. Observing the cardinality of the sets $\Psi_j^{\square}$, $\widetilde{\Psi}_j^{\square}$ biorthogonality implies the assertion. ∎

The refinement matrices $\mathbf{M}_{j,1}^{\square}$ and $\widetilde{\mathbf{M}}_{j,1}^{\square}$ are computed by

$$\mathbf{M}_{j,1}^{\square} = \begin{bmatrix} \mathbf{M}_{j,1}^{[0,1]} \otimes \mathbf{M}_{j,0}^{[0,1]} \\ \mathbf{I}^{|\Delta_{j+1}^{[0,1]}|} \otimes \mathbf{M}_{j,1}^{[0,1]} \end{bmatrix}, \qquad \widetilde{\mathbf{M}}_{j,1}^{\square} = \begin{bmatrix} \widetilde{\mathbf{M}}_{j,1}^{[0,1]} \otimes \widetilde{\mathbf{M}}_{j,0}^{[0,1]} \\ \mathbf{I}^{|\Delta_{j+1}^{[0,1]}|} \otimes \widetilde{\mathbf{M}}_{j,1}^{[0,1]} \end{bmatrix}.$$

Thus, we obtain two types of wavelets on $\square$, cf. Figures 2.1 and 2.2. The first type is the tensor product $\psi_{j,k}^{[0,1]} \otimes \phi_{j,l}^{[0,1]}$. The second type is the tensor product $\phi_{j+1,k}^{[0,1]} \otimes \psi_{j,l}^{[0,1]}$. Notice that these wavelets have a very small support in comparison with the previously introduced wavelets, since a scaling function of the fine grid $j+1$ appears in the first coordinate. Additionally, the number of wavelets of type two is nearly twice as much as the number of wavelets of type one.

REMARK 2.2. *This construction is highly attractive in higher dimensions since each wavelet coincides only in one coordinate with a wavelet from the interval while in the other coordinates only scaling functions of the levels j and $j+1$ appear, cf. [23] for further details.*

2.3. Wavelets on Manifolds. In this subsection, we employ a domain decomposition strategy and introduce a family of parametric representations which describe the given manifold. Subsequently, the wavelets on the manifold are defined via the parametrization. We consider two different constructions for wavelets on manifolds. The first one leads to wavelets which are defined on each patch individually. The second and more complicated one yields globally continuous wavelets.

2.3.1. Parametric Representations of Manifolds. We subdivide the given manifold $\Gamma \in \mathbb{R}^3$ into several *patches*

$$\Gamma = \bigcup_{i=1}^{M} \Gamma_i, \qquad \Gamma_i = \gamma_i(\square), \qquad i = 1, 2, \ldots, M, \tag{2.7}$$

such that each $\gamma_i : \square \to \Gamma_i$ defines a diffeomorphism of $\square$ onto Γ_i. The intersection $\Gamma_i \cap \Gamma_{i'}$, $i \neq i'$, of the patches Γ_i and $\Gamma_{i'}$ is supposed to be either $\emptyset$ or a common edge or vertex.

A mesh of level j on Γ is induced by dyadic subdivisions of depth j of the unit cube into 4^j cubes. This generates $4^j M$ *elements*. For obtaining a regular mesh of Γ the parametric representation is subjected to the following matching condition. For all $\mathbf{x} \in \Gamma_i \cap \Gamma_{i'}$ exists a bijective, affine mapping $\Xi : \square \to \square$ such that $\gamma_i(\mathbf{s}) = (\gamma_{i'} \circ \Xi)(\mathbf{s}) = \mathbf{x}$ for $\mathbf{s} \in \square$ with $\gamma_i(\mathbf{s}) = \mathbf{x}$, cf. Figure 2.3. Unfortunately, this essential supposition restricts the choice of the parametric representation.

The canonical inner product in $L^2(\Gamma)$ is given by

$$(u, v)_{L^2(\Gamma)} = \int_{\Gamma} u(\mathbf{x}) v(\mathbf{x}) d\sigma_{\mathbf{x}} = \sum_{i=1}^{M} \int_{\square} u\big(\gamma_i(\mathbf{s})\big) v\big(\gamma_i(\mathbf{s})\big) \kappa_i(\mathbf{s}) d\mathbf{s} \tag{2.8}$$

where $\kappa_i(\mathbf{s})$ denotes the surface measure. The corresponding Sobolev spaces are indicated by $H^s(\Gamma)$. Of course, depending on the global smoothness of the surface, the range of permitted $s \in \mathbb{R}$ is limited to $s \in (-s_\Gamma, s_\Gamma)$. An important role is played by the following modified inner product which arises from (2.8) by omitting the surface measure

$$\langle u, v \rangle = \sum_{i=1}^{M} (u \circ \gamma_i, v \circ \gamma_i)_{L^2(\square)} = \sum_{i=1}^{M} \int_{\square} u\big(\gamma_i(\mathbf{s})\big) v\big(\gamma_i(\mathbf{s})\big) d\mathbf{s}. \tag{2.9}$$

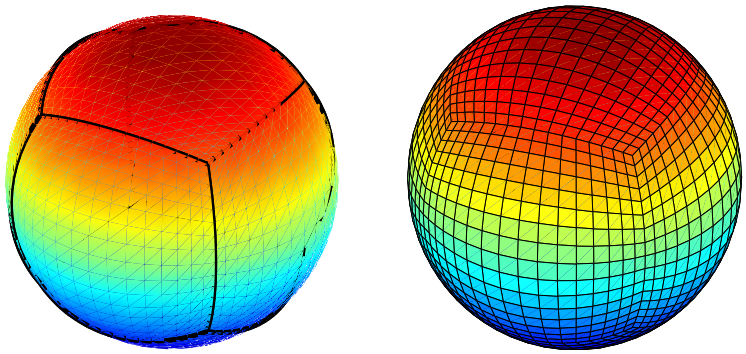

FIG. 2.3. *The parametric representation of the unit sphere is obtained by projecting it onto the cube* $[-1,1]^3$*, which yields six patches (left). On the right hand side one figures out the partition on the level* $j = 4$.

In $L^2(\Gamma)$ both inner products define equivalent norms $\langle u, u\rangle \sim (u,u)_{L^2(\Gamma)}$. However, in general, even on smooth surfaces, κ_i is not continuous accross the interfaces of the patches, i.e., for $\gamma_i(\mathbf{s}) = \gamma_{i'}(\mathbf{s}') = \mathbf{x} \in \Gamma_i \cap \Gamma_{i'}$ one has

$$\kappa_i(\mathbf{s}) \neq \kappa_{i'}(\mathbf{s}'). \tag{2.10}$$

In the next subsections, the biorthogonal multiresolution on Γ is constructed with respect to the modified inner product. Thus, due to (2.10), the norm equivalence with respect to the canonical Sobolev spaces $H^s(\Gamma)$ is limited from below by $s = -1/2$.

2.3.2. Patchwise smooth Wavelet Bases. If the wavelet basis is not required to be globally continuous, one may employ wavelet bases defined on each patch individually. This strategy reflects the canonical one for the piecewise constants. But in the case of higher order ansatz functions we obtain double nodes along the edges of intersecting patches. This leads to more degrees of freedom than in the case of global continuity.

The primal scaling functions and wavelets are given by

$$\phi^{\Gamma_i}_{j,\mathbf{k}}(\mathbf{x}) := \begin{cases} \phi^{\square}_{j,\mathbf{k}}\big(\gamma_i^{-1}(\mathbf{x})\big), & \mathbf{x} \in \Gamma_i, \\ 0, & \text{else}, \end{cases} \qquad \psi^{\Gamma_i}_{j,\mathbf{k}}(\mathbf{x}) := \begin{cases} \psi^{\square}_{j,\mathbf{k}}\big(\gamma_i^{-1}(\mathbf{x})\big), & \mathbf{x} \in \Gamma_i, \\ 0, & \text{else}. \end{cases}$$

Setting $\Phi^{\Gamma_i}_j = \big[\phi^{\Gamma_i}_{j,\mathbf{k}}\big]_{\mathbf{k}\in\Delta^{\square}_j}$ and $\Psi^{\Gamma_i}_j = \big[\psi^{\Gamma_i}_{j,\mathbf{k}}\big]_{\mathbf{k}\in\nabla^{\square}_j}$, the collections of scaling functions and wavelets on Γ are defined by $\Phi^{\Gamma}_j := \big[\Phi^{\Gamma_i}_j\big]_{i=1}^M$ and $\Psi^{\Gamma}_j := \big[\Psi^{\Gamma_i}_j\big]_{i=1}^M$. Obviously, the refinement matrices with $\Phi^{\Gamma}_j = \Phi^{\Gamma}_{j+1}\mathbf{M}^{\Gamma}_{j,0}$ and $\Psi^{\Gamma}_j = \Phi^{\Gamma}_{j+1}\mathbf{M}^{\Gamma}_{j,1}$ are obtained by

$$\mathbf{M}^{\Gamma}_{j,0} = \operatorname{diag}\big(\underbrace{\mathbf{M}^{\square}_{j,0}, \ldots, \mathbf{M}^{\square}_{j,0}}_{M \text{ times}}\big), \qquad \mathbf{M}^{\Gamma}_{j,1} = \operatorname{diag}\big(\underbrace{\mathbf{M}^{\square}_{j,1}, \ldots, \mathbf{M}^{\square}_{j,1}}_{M \text{ times}}\big).$$

Clearly, the spaces $V^{\Gamma}_j := \operatorname{span}\Phi^{\Gamma}_j$ are nested. In addition, we find $V^{\Gamma}_{j+1} = V^{\Gamma}_j \oplus W^{\Gamma}_j$, where $W^{\Gamma}_j := \operatorname{span}\Psi^{\Gamma}_j$. Proceeding analogously on the dual side yields a multiresolution on Γ which is biorthogonal with respect to the modified inner product (2.9).

In order to formulate the properties of the wavelets defined by (1.12) we introduce new function spaces on Γ. For arbitrary $s \geq 0$ we define the Sobolev spaces $H^s_{\langle\cdot,\cdot\rangle}(\Gamma)$ as closure of all patchwise C^∞-functions on Γ with respect to the norm

$$\|v\|_{H^s_{\langle\cdot,\cdot\rangle}(\Gamma)} := \sum_{i=1}^{M} \|v \circ \gamma_i\|_{H^s(\square)}\,.$$

The space $L^2_{\langle\cdot,\cdot\rangle}(\Gamma)$ indicates as usual the Sobolev space $H^0_{\langle\cdot,\cdot\rangle}(\Gamma)$. The Sobolev spaces of negative order, that is $H^{-s}_{\langle\cdot,\cdot\rangle}(\Gamma)$, are defined as the duals of $H^s_{\langle\cdot,\cdot\rangle}(\Gamma)$ with respect to the modified inner product (2.9). Consequently, $H^{-s}_{\langle\cdot,\cdot\rangle}(\Gamma)$ is equipped by the norm

$$\|v\|_{H^{-s}_{\langle\cdot,\cdot\rangle}(\Gamma)} := \sup_{w \in H^s_{\langle\cdot,\cdot\rangle}(\Gamma)} \frac{\langle v, w\rangle}{\|w\|_{H^s_{\langle\cdot,\cdot\rangle}(\Gamma)}}.$$

The subsequent proposition proven in [16] states that we obtain all important properties of the univariate case with respect to the modified inner product.

PROPOSITION 2.3. *The collection of wavelets Ψ^Γ and $\widetilde{\Psi}^\Gamma$ form biorthogonal Riesz bases in $L^2_{\langle\cdot,\cdot\rangle}(\Gamma)$. The primal wavelets satisfy the cancellation property* (1.4) *with parameter $\widetilde{d}$ with respect to the modified inner product. Moreover, the norm equivalences* (1.13) *hold with $\gamma = \gamma^{\mathbb{R}}$ and $\widetilde{\gamma}^{\mathbb{R}}$ with respect to the spaces $H^s_{\langle\cdot,\cdot\rangle}(\Gamma)$*

REMARK 2.4. *Of course, the cancellation property* (1.4) *with parameter $\widetilde{d}$ holds also with respect to the canonical inner product, since the wavelets are supported on a single patch. Since the Sobolev spaces $H^s(\Gamma)$ and $H^s_{\langle\cdot,\cdot\rangle}(\Gamma)$ are isomorphic in the range $s \in \big(-\frac{1}{2}, \frac{1}{2}\big)$, see [16] for details, the norm equivalences with respect to the canonical Sobolev spaces $H^s(\Gamma)$ are valid with $\gamma = \min\{1/2, \gamma^R\}$ and $\widetilde{\gamma} = \min\{1/2, \widetilde{\gamma}^R\}$. In particular, the collections Ψ^Γ and $\widetilde{\Psi}^\Gamma$ are Riesz bases.*

2.3.3. Globally Continuous Wavelet Bases. The construction of globally continuous wavelets on Γ is based on the simplified tensor product wavelets. Both, the scaling functions and the stable completion, are required to satisfy the conditions specified in Subsection 2.1. In order to realize the continuity we perform a gluing technique along the interfaces of intersecting patches.

We introduce first some further notation since we have to deal with local indices and functions defined on the parameter domain $\square$ as well as global indices and functions on the surface Γ. To this end, it is convenient to identify the basis functions with physical grid points on the mesh on the unit square, i.e. we employ a bijective mapping $q_j : \Delta_j^\square \to \square$ in order to redefine our index sets on the unit square. This mapping should identify the boundary functions with points on $\partial\square$. Moreover, it should preserve the symmetry, that is, in view of (2.3), given any affine mapping $\Xi : \square \to \square$, there holds

$$\Phi_j^\square = \Phi_j^\square \circ \Xi, \qquad \breve{\Psi}_j^\square = \breve{\Psi}_j^\square \circ \Xi, \qquad \widetilde{\Phi}_j^\square = \widetilde{\Phi}_j^\square \circ \Xi, \qquad \widetilde{\Psi}_j^\square = \widetilde{\Psi}_j^\square \circ \Xi. \tag{2.11}$$

Then, the boundary conditions (2.1) and (2.2) imply

$$\begin{aligned} &\phi^\square_{j,\mathbf{k}}\Big|_{\partial\square} \equiv \widetilde{\phi}^\square_{j,\mathbf{k}}\Big|_{\partial\square} \equiv 0, && \mathbf{k} \in \Delta_j^\square \cap \square^\circ, \\ &\breve{\psi}^\square_{j,\mathbf{k}}\Big|_{\partial\square} \equiv 0, && \mathbf{k} \in \nabla_j^\square \cap \square^\circ. \end{aligned}$$

Hence, all functions corresponding to the indices $\mathbf{k}$ lying in the interior of $\square$ satisfy zero boundary conditions. In the case of piecewise bilinears the mapping q_j is simply defined by $q_j(\mathbf{k}) = 2^{-j}\mathbf{k}$. For the general case we refer to [16, 23].

A given point $\mathbf{x} \in \Gamma$ might have several representations

$$\mathbf{x} = \gamma_{i_1}(\mathbf{s}_1) = \ldots = \gamma_{i_{r(\mathbf{x})}}(\mathbf{s}_{r(\mathbf{x})})$$

if $\mathbf{x}$ belongs to different patches $\Gamma_{i_1}, \ldots, \Gamma_{i_{r(\mathbf{x})}}$. Of course, this occurs only if $\mathbf{x}$ lies on a edge or vertex of a patch. We count the number of preimages of a given point $\mathbf{x} \in \Gamma$ by the function $r : \Gamma \to \mathbb{N}$,

$$r(\mathbf{x}) := \big|\big\{i \in \{1, 2, \ldots, M\} : \mathbf{x} \in \Gamma_i\big\}\big|. \tag{2.12}$$

Clearly, one has $r(\mathbf{x}) \geq 1$, where $r(\mathbf{x}) = 1$ holds for all $\mathbf{x}$ lying in the interior of the patches Γ_i. Moreover, $r(\mathbf{x}) = 2$ for all $\mathbf{x}$ which belong to an edge and are different from a vertex.

Next, given two points $\mathbf{x}, \mathbf{y} \in \Gamma$, the function $c : \Gamma \times \Gamma \to \mathbb{N}$ defined by

$$c(\mathbf{x}, \mathbf{y}) := \big|\big\{i \in \{1, 2, \ldots, M\} : \mathbf{x} \in \Gamma_i \wedge \mathbf{y} \in \Gamma_i\big\}\big| \tag{2.13}$$

counts the number of patches Γ_i containing both points together.

Now, on Γ, the index sets are given by physical grid points on the surface

$$\Delta_j^\Gamma := \big\{\gamma_i(\mathbf{k}) : \mathbf{k} \in \Delta_j^\square,\ i \in \{1, 2, \ldots, M\}\big\}, \qquad \nabla_j^\Gamma := \Delta_{j+1}^\Gamma \setminus \Delta_j^\Gamma. \tag{2.14}$$

The gluing along the intersections of the patches is performed as follows. According to [16], the scaling functions $\Phi_j^\Gamma := \big[\phi_{j,\boldsymbol{\xi}}^\Gamma\big]_{\boldsymbol{\xi} \in \Delta_j^\Gamma}$ and $\widetilde{\Phi}_j^\Gamma := \big[\widetilde{\phi}_{j,\boldsymbol{\xi}}^\Gamma\big]_{\boldsymbol{\xi} \in \Delta_j^\Gamma}$ are defined by

$$\begin{aligned}
\phi_{j,\boldsymbol{\xi}}^\Gamma(\mathbf{x}) &= \begin{cases} \phi_{j,\mathbf{k}}^\square\big(\gamma_i^{-1}(\mathbf{x})\big), & \exists (i,\mathbf{k}) : \gamma_i(\mathbf{k}) = \boldsymbol{\xi} \wedge \mathbf{x} \in \Gamma_i, \\ 0, & \text{elsewhere.} \end{cases} \\
\widetilde{\phi}_{j,\boldsymbol{\xi}}^\Gamma(\mathbf{x}) &= \begin{cases} \frac{1}{r(\boldsymbol{\xi})}\widetilde{\phi}_{j,\mathbf{k}}^\square\big(\gamma_i^{-1}(\mathbf{x})\big), & \exists (i,\mathbf{k}) : \gamma_i(\mathbf{k}) = \boldsymbol{\xi} \wedge \mathbf{x} \in \Gamma_i, \\ 0, & \text{elsewhere.} \end{cases}
\end{aligned} \tag{2.15}$$

On the primal side, this definition reflects the canonical strategy. On the dual side, the strategy is analogously except for normalization, for a visualisation see also Figure 2.4. The normalization factor ensures biorthogonality with respect to the modified inner product (2.9), i.e. $\langle \Phi_j^\Gamma, \widetilde{\Phi}_j^\Gamma \rangle = \mathbf{I}$. The scaling functions are refinable Riesz bases of the spaces $V_j^\Gamma := \operatorname{span} \Phi_j^\Gamma$ and $\widetilde{V}_j^\Gamma := \operatorname{span} \widetilde{\Phi}_j^\Gamma$.

The two scale relations (1.16) associated with these scaling functions are given by

$$\big[\mathbf{M}_{j,0}^\Gamma\big]_{\boldsymbol{\xi}',\boldsymbol{\xi}} = \begin{cases} \big[\mathbf{M}_{j,0}^\square\big]_{\mathbf{k}',\mathbf{k}}, & \exists (i,\mathbf{k},\mathbf{k}') : \boldsymbol{\xi} = \gamma_i(\mathbf{k}) \wedge \boldsymbol{\xi}' = \gamma_i(\mathbf{k}'), \\ 0, & \text{elsewhere,} \end{cases} \tag{2.16}$$

$$\big[\widetilde{\mathbf{M}}_{j,0}^\Gamma\big]_{\boldsymbol{\xi}',\boldsymbol{\xi}} = \begin{cases} \frac{c(\boldsymbol{\xi},\boldsymbol{\xi}')}{r(\boldsymbol{\xi})}\big[\widetilde{\mathbf{M}}_{j,0}^\square\big]_{\mathbf{k}',\mathbf{k}}, & \exists (i,\mathbf{k},\mathbf{k}') : \boldsymbol{\xi} = \gamma_i(\mathbf{k}) \wedge \boldsymbol{\xi}' = \gamma_i(\mathbf{k}'), \\ 0, & \text{elsewhere.} \end{cases} \tag{2.17}$$

This formula has been proven in [16] with the weight factor $\frac{r(\boldsymbol{\xi}')}{r(\boldsymbol{\xi})}$ instead of $\frac{c(\boldsymbol{\xi},\boldsymbol{\xi}')}{r(\boldsymbol{\xi})}$. But the case $r(\boldsymbol{\xi}') \neq c(\boldsymbol{\xi},\boldsymbol{\xi}')$ appears

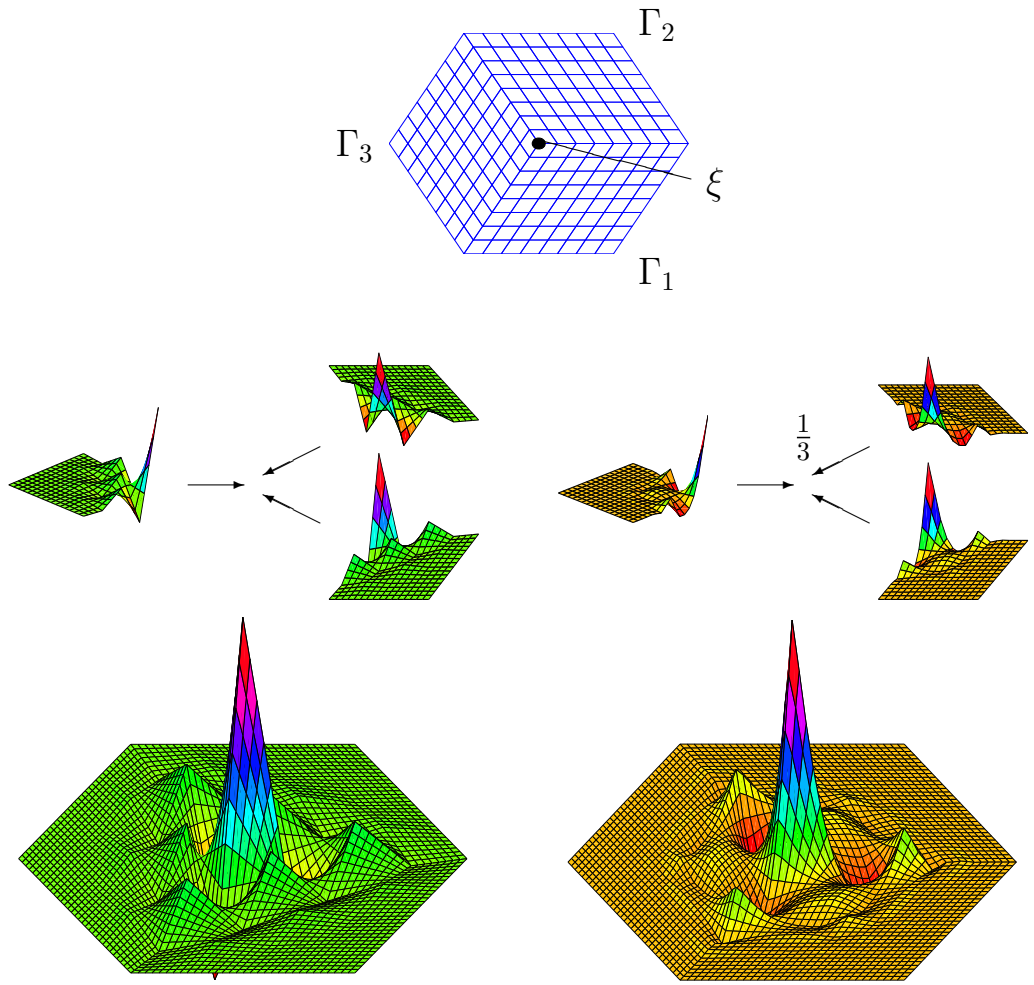

FIG. 2.4. *The primal (left) and the dual (right) generator on a degenerated vertex in the case* $(d, \widetilde{d}) = (2, 4)$.

– either if $\boldsymbol{\xi}'$ is a vertex and $\boldsymbol{\xi}' \neq \boldsymbol{\xi}$

– or $\boldsymbol{\xi}'$ lies on a certain edge and $\boldsymbol{\xi}$ does not,

or vice versa. But in these cases the boundary conditions (2.1) imply $\big[\widetilde{\mathbf{M}}^{\Gamma}_{j,0}\big]_{\boldsymbol{\xi}',\boldsymbol{\xi}} = 0$.

The stable completion $\breve{\Psi}_j = \big[\breve{\psi}^{\Gamma}_{j,\boldsymbol{\xi}}\big]_{\boldsymbol{\xi}\in\nabla^{\Gamma}_j}$ is defined analogously to the primal scaling functions. In accordance with [16] one has

$$\breve{\psi}^{\Gamma}_{j,\boldsymbol{\xi}}(\mathbf{x}) = \begin{cases} \breve{\psi}^{\square}_{j,\mathbf{k}}\big(\gamma_i^{-1}(\mathbf{x})\big), & \exists (i,\mathbf{k}) : \gamma_i(\mathbf{k}) = \boldsymbol{\xi} \wedge \mathbf{x} \in \Gamma_i, \\ 0, & \text{elsewhere.} \end{cases} \tag{2.18}$$

Consequently, the refinement matrix is determined analogously to $\mathbf{M}^{\Gamma}_{j,0}$ by

$$\big[\breve{\mathbf{M}}^{\Gamma}_{j,1}\big]_{\boldsymbol{\xi}',\boldsymbol{\xi}} = \begin{cases} \big[\breve{\mathbf{M}}^{\square}_{j,1}\big]_{\mathbf{k}',\mathbf{k}}, & \exists (i,\mathbf{k},\mathbf{k}') : \boldsymbol{\xi} = \gamma_i(\mathbf{k}) \wedge \boldsymbol{\xi}' = \gamma_i(\mathbf{k}'), \\ 0, & \text{elsewhere.} \end{cases} \tag{2.19}$$

The dual wavelets $\widetilde{\Psi}_j^\Gamma := \big[\widetilde{\psi}_{j,\boldsymbol{\xi}}^\Gamma\big]_{\boldsymbol{\xi}\in\nabla_j^\Gamma}$ are obtained by their refinement relation (1.16), where

$$\big[\widetilde{\mathbf{M}}_{j,1}^\Gamma\big]_{\boldsymbol{\xi}',\boldsymbol{\xi}} = \begin{cases} \frac{c(\boldsymbol{\xi},\boldsymbol{\xi}')}{r(\boldsymbol{\xi})}\big[\widetilde{\mathbf{M}}_{j,1}^\square\big]_{\mathbf{k}',\mathbf{k}}, & \exists(i,\mathbf{k},\mathbf{k}') : \boldsymbol{\xi} = \gamma_i(\mathbf{k}) \wedge \boldsymbol{\xi}' = \gamma_i(\mathbf{k}'), \\ 0, & \text{elsewhere}, \end{cases} \tag{2.20}$$

cf. [16, 23]. A closed expression of the matrix $\mathbf{L}_j^\Gamma := \big(\widetilde{\mathbf{M}}_{j,0}^\Gamma\big)^T\breve{\mathbf{M}}_{j,1}^\Gamma$ is crucial for the implementation of the discrete wavelet transform. In fact, the next theorem confirms the existence of an explicit formula.

THEOREM 2.5. *The entries of the matrix* $\mathbf{L}_j^\Gamma = \big(\widetilde{\mathbf{M}}_{j,0}^\Gamma\big)^T\breve{\mathbf{M}}_{j,1}^\Gamma$ *are given by*

$$\big[\mathbf{L}_j^\Gamma\big]_{\boldsymbol{\xi}',\boldsymbol{\xi}} = \begin{cases} \frac{c(\boldsymbol{\xi},\boldsymbol{\xi}')}{r(\boldsymbol{\xi}')}\big[\mathbf{L}_j^\square\big]_{\mathbf{k}',\mathbf{k}}, & \exists(i,\mathbf{k},\mathbf{k}') : \boldsymbol{\xi} = \gamma_i(\mathbf{k}) \wedge \boldsymbol{\xi}' = \gamma_i(\mathbf{k}'), \\ 0, & \textit{elsewhere}. \end{cases} \tag{2.21}$$

Proof. Let $\boldsymbol{\xi} \in \nabla_j^\Gamma$ and $\boldsymbol{\xi}' \in \Delta_j^\Gamma$ be arbitrarily but fixed. A single entry of $\mathbf{L}_j^\Gamma$ is given with respect to the modified scalar product (2.9) by $\big[\mathbf{L}_j^\Gamma\big]_{\boldsymbol{\xi}',\boldsymbol{\xi}} = \langle\widetilde{\phi}_{j,\boldsymbol{\xi}'}^\Gamma, \breve{\psi}_{j,\boldsymbol{\xi}}^\Gamma\rangle$. Inserting the definitions of $\widetilde{\phi}_{j,\boldsymbol{\xi}'}^\Gamma$ and $\breve{\psi}_{j,\boldsymbol{\xi}}^\Gamma$, that is (2.15) and (2.18), yields

$$\big[\mathbf{L}_j^\Gamma\big]_{\boldsymbol{\xi}',\boldsymbol{\xi}} = \sum_{(i,\mathbf{k},\mathbf{k}'):\boldsymbol{\xi}=\gamma_i(\mathbf{k})\wedge\boldsymbol{\xi}'=\gamma_i(\mathbf{k}')} \frac{1}{r(\boldsymbol{\xi}')}\big(\widetilde{\phi}_{j,\mathbf{k}'}^\square, \breve{\psi}_{j,\mathbf{k}}^\square\big)_{L^2(\square)}. \tag{2.22}$$

Of course, we deduce that $\big[\mathbf{L}_j^\Gamma\big]_{\boldsymbol{\xi}',\boldsymbol{\xi}} = 0$ if there exists no triple $(i,\mathbf{k},\mathbf{k}')$ with $\boldsymbol{\xi} = \gamma_i(\mathbf{k})$ and $\boldsymbol{\xi}' = \gamma_i(\mathbf{k}')$, i.e. if $c(\boldsymbol{\xi},\boldsymbol{\xi}') = 0$, which proves the second case in (2.21). Next, we assume $c(\boldsymbol{\xi},\boldsymbol{\xi}') > 0$. Then, there exist $c(\boldsymbol{\xi},\boldsymbol{\xi}')$ different tuples $(i_l,\mathbf{k}_l,\mathbf{k}_l')$ with $\boldsymbol{\xi} = \gamma_{i_l}(\mathbf{k}_l)$ and $\boldsymbol{\xi}' = \gamma_{i_l}(\mathbf{k}')$, $l = 1,2,\ldots,c(\boldsymbol{\xi},\boldsymbol{\xi}')$. The symmetry relations (2.11) imply that

$$\big(\widetilde{\phi}_{j,\mathbf{k}_1'}^\square, \breve{\psi}_{j,\mathbf{k}_1}^\square\big)_{L^2(\square)} = \ldots = \big(\widetilde{\phi}_{j,\mathbf{k}'_{c(\boldsymbol{\xi},\boldsymbol{\xi}')}}^\square, \breve{\psi}_{j,\mathbf{k}_{c(\boldsymbol{\xi},\boldsymbol{\xi}')}}^\square\big)_{L^2(\square)} = \big[\mathbf{L}_j^\square\big]_{\mathbf{k}',\mathbf{k}}.$$

Therefore, we conclude the validity of (2.21). ∎

As an immediate consequence of this theorem, we end up with a black box algorithm for the computation of the discrete wavelet transform. Although the definitions of the refinement matrices seem to be very technical, the implementation of the discrete wavelet transform is rather canonical as the algorithms 1 and 2 confirm.

For arbitrary $s \geq 0$ let the Sobolev spaces $H_{\langle\cdot,\cdot\rangle}^s(\Gamma)$ be the closure of all *globally continuous*, patchwise C^∞-functions on Γ with respect to the norm

$$\|v\|_{H_{\langle\cdot,\cdot\rangle}^s(\Gamma)} := \sum_{i=1}^M \|v\circ\gamma_i\|_{H^s(\square)}.$$

The space $L_{\langle\cdot,\cdot\rangle}^2(\Gamma)$ indicates as usual the Sobolev space $H_{\langle\cdot,\cdot\rangle}^0(\Gamma)$. The Sobolev space $H_{\langle\cdot,\cdot\rangle}^{-s}(\Gamma)$, $s < 0$, is defined as the dual of $H_{\langle\cdot,\cdot\rangle}^s(\Gamma)$ with respect to the modified inner product (2.9), i.e.

$$\|v\|_{H_{\langle\cdot,\cdot\rangle}^{-s}(\Gamma)} := \sup_{w\in H_{\langle\cdot,\cdot\rangle}^s(\Gamma)} \frac{\langle v,w\rangle}{\|w\|_{H_{\langle\cdot,\cdot\rangle}^s(\Gamma)}}.$$

Algorithm 1 This algorithm computes the two scale decomposition $\widetilde{\Phi}^{\Gamma}_{j+1}\mathbf{a}^{(j+1)} = \widetilde{\Phi}^{\Gamma}_{j}\mathbf{a}^{(j)} + \widetilde{\Psi}^{\Gamma}_{j}\mathbf{b}^{(j)}$, where $\mathbf{a}^{(j)} = \big[a^{(j)}_{\boldsymbol{\xi}}\big]_{\boldsymbol{\xi}\in\Delta^{\Gamma}_{j}}$ and $\mathbf{b}^{(j)} = \big[b^{(j)}_{\boldsymbol{\xi}}\big]_{\boldsymbol{\xi}\in\nabla^{\Gamma}_{j}}$.

initialization: $\mathbf{a}^{(j)} := \mathbf{b}^{(j)} := \mathbf{0}$
for $i = 1$ **to** M **do begin**
  for all $\mathbf{k} \in \Delta^{\square}_{j}$ **do begin** C: compute coefficients of $\widetilde{\Phi}^{\Gamma}_{j}$
    for all $\mathbf{k}' \in \Delta^{\square}_{j+1}$ **do begin**
      $a^{(j)}_{\gamma_i(\mathbf{k})} = a^{(j)}_{\gamma_i(\mathbf{k})} + \big[\mathbf{M}^{\square}_{j,0}\big]_{\mathbf{k}',\mathbf{k}} a^{(j+1)}_{\gamma_i(\mathbf{k}')}/r\big(\gamma_i(\mathbf{k})\big)$
  end, end
  for all $\mathbf{k} \in \nabla^{\square}_{j}$ **do begin** C: compute coefficients of $\widetilde{\Psi}^{\Gamma}_{j}$
    for all $\mathbf{k}' \in \Delta^{\square}_{j+1}$ **do begin**
      $b^{(j)}_{\gamma_i(\mathbf{k})} = b^{(j)}_{\gamma_i(\mathbf{k})} + \big[\mathbf{M}^{\square}_{j,1}\big]_{\mathbf{k}',\mathbf{k}} a^{(j+1)}_{\gamma_i(\mathbf{k}')}/r\big(\gamma_i(\mathbf{k})\big)$
end, end, end.

Algorithm 2 This algorithm computes the two scale decomposition $\Phi^{\Gamma}_{j+1}\mathbf{a}^{(j+1)} = \Phi^{\Gamma}_{j}\mathbf{a}^{(j)} + \Psi^{\Gamma}_{j}\mathbf{b}^{(j)}$, where $\mathbf{a}^{(j)} = \big[a^{(j)}_{\boldsymbol{\xi}}\big]_{\boldsymbol{\xi}\in\Delta^{\Gamma}_{j}}$ and $\mathbf{b}^{(j)} = \big[b^{(j)}_{\boldsymbol{\xi}}\big]_{\boldsymbol{\xi}\in\nabla^{\Gamma}_{j}}$.

initialization: $\mathbf{a}^{(j)} := \mathbf{b}^{(j)} := \mathbf{0}$
for $i = 1$ **to** M **do begin**
  for all $\mathbf{k} \in \Delta^{\square}_{j}$ **do begin** C: compute coefficients of Φ^{Γ}_{j}
    for all $\mathbf{k}' \in \Delta^{\square}_{j+1}$ **do begin**
      $a^{(j)}_{\gamma_i(\mathbf{k})} = a^{(j)}_{\gamma_i(\mathbf{k})} + \big[\mathbf{M}^{\square}_{j,0}\big]_{\mathbf{k}',\mathbf{k}} a^{(j+1)}_{\gamma_i(\mathbf{k}')}/r\big(\gamma_i(\mathbf{k}')\big)$
  end, end
  for all $\mathbf{k} \in \nabla^{\square}_{j}$ **do begin** C: compute coefficients of $\breve{\Psi}^{\Gamma}_{j}$
    for all $\mathbf{k}' \in \Delta^{\square}_{j+1}$ **do begin**
      $b^{(j)}_{\gamma_i(\mathbf{k})} = b^{(j)}_{\gamma_i(\mathbf{k})} + \big[\mathbf{M}^{\square}_{j,1}\big]_{\mathbf{k}',\mathbf{k}} a^{(j+1)}_{\gamma_i(\mathbf{k}')}/r\big(\gamma_i(\mathbf{k}')\big)$
end, end, end
for $i = 1$ **to** M **do begin**
  for all $\mathbf{k} \in \nabla^{\square}_{j}$ **do begin** C: add scaling functions to $\breve{\Psi}^{\Gamma}_{j}$
    for all $\mathbf{k}' \in \Delta^{\square}_{j}$ **do begin**
      $b^{(j)}_{\gamma_i(\mathbf{k})} = b^{(j)}_{\gamma_i(\mathbf{k})} - \big[\mathbf{L}^{\square}_{j}\big]_{\mathbf{k}',\mathbf{k}} a^{(j)}_{\gamma_i(\mathbf{k}')}/r\big(\gamma_i(\mathbf{k}')\big)$
end, end, end.

PROPOSITION 2.6. *The collection of wavelets Ψ^Γ and $\widetilde{\Psi}^\Gamma$ form biorthogonal Riesz bases in $L^2_{\langle\cdot,\cdot\rangle}(\Gamma)$. The primal wavelets satisfy the cancellation property* (1.4) *with parameter $\widetilde{d}$ with respect to the modified inner product. Moreover, the norm equivalences* (1.13) *hold with $\gamma = \gamma^{\mathbb{R}}$ and $\widetilde{\gamma}^{\mathbb{R}}$ with respect to the spaces $H^s_{\langle\cdot,\cdot\rangle}(\Gamma)$* Considering the canonical inner product, the cancellation property is in general not satisfied if the wavelet is supported on several patches. For such wavelets the cancellation property is true only if the surface measure is continuous across the interfaces of intersecting patches.

According to [16], the Sobolev spaces $H^s(\Gamma)$ and $H^s_{\langle\cdot,\cdot\rangle}(\Gamma)$ are isomorphic in the range $s \in (-\frac{1}{2}, \min\{\frac{3}{2}, s_\Gamma\})$. This yields that the norm equivalences (1.13) with respect to the canonical Sobolev spaces are valid with $\gamma := \min\{\frac{3}{2}, \gamma^{\mathbb{R}}\}$ and $\widetilde{\gamma} := \min\{\frac{1}{2}, \widetilde{\gamma}^{\mathbb{R}}\}$. For $s = 0$ we obtain the Riesz property of the collections Ψ^Γ and $\widetilde{\Psi}^\Gamma$ with respect to the canonical inner product.

3. Numerical Results. This section is dedicated to numerical examples in order to demonstrate the wavelet Galerkin schemes based on the different wavelet constructions. Firstly, we compute a Dirichlet problem. We use the indirect formulation for the double layer operator which gives a Fredholm's integral equation of the second kind. This is approximated by using piecewise constant wavelets. Secondly, we solve a Neumann problem employing the indirect formulation for the hypersingular operator. The discretization requires globally continuous piecewise linear wavelets. We mention that both problems are chosen such that the solutions are known analytically in order to measure the error of method.

3.1. Dirichlet Problem. For a given $f \in H^{1/2}(\Gamma)$ we consider an interior Dirichlet problem, i.e., we seek $u \in H^1(\Omega)$ such that

$$\Delta u = 0 \text{ in } \Omega, \qquad u = f \text{ on } \Gamma. \tag{3.1}$$

The domain Ω is described by the set difference of the cube $[-1,1]^3$ and three cylinders with radii 0.5, cf. Figure 3.1. The boundary Γ is parametrized via 48 patches. Choosing the harmonical function $u(\mathbf{x}) = 4x^2 - 3y^2 - z^2$ and setting $f := u|_\Gamma$ the problem (3.1) has the unique solution u.

Employing the double layer operator

$$(\mathcal{K}\rho)(\mathbf{x}) := \frac{1}{4\pi} \int_\Gamma \frac{\partial}{\partial \mathbf{n}_\mathbf{y}} \frac{1}{\|\mathbf{x}-\mathbf{y}\|^2} \rho(\mathbf{y}) d\sigma_\mathbf{y}, \quad \mathbf{x} \in \Gamma, \tag{3.2}$$

yields the Fredholm integral equation of the second kind

$$\big(\mathcal{K} - \tfrac{1}{2} I\big)\rho = f \quad \text{on } \Gamma.$$

Herein, the operator on the left hand side defines an operator of the order 0. We discretize this equation by piecewise constant wavelets with three vanishing moments which is in accordance with (1.14). In order to compare the different constructions from Subsection 2.2 we compute the solution with respect to all wavelet bases presented in Figure 2.1.

The density ρ given by the boundary integral equation (3.2) yields the solution u of the Dirichlet problem by application of the double layer operator

$$u = \mathcal{K}\rho \quad \text{in } \Omega. \tag{3.3}$$

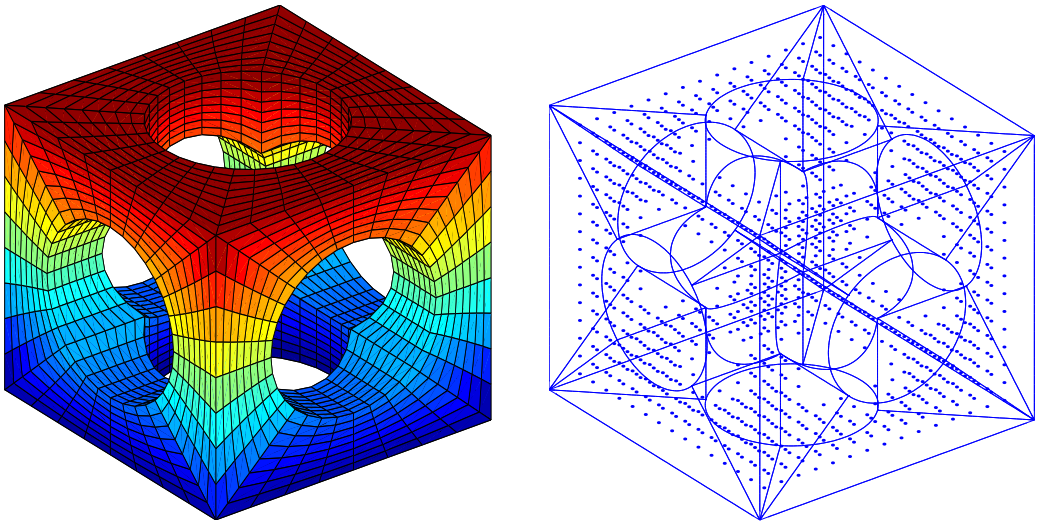

FIG. 3.1. *The mesh on the surface* Γ *and the evaluation points* $\mathbf{x}_i$ *of the potential.*

We denote the discrete counterparts by

$$\mathbf{u} := [u(\mathbf{x}_i)], \quad \mathbf{u}_J^\phi := [(\mathcal{K}\rho_J^\phi)(\mathbf{x}_i)], \quad \mathbf{u}_J^\psi := [(\mathcal{K}\rho_J^\psi)(\mathbf{x}_i)], \tag{3.4}$$

where the evaluation points $\mathbf{x}_i$ are specified in Figure 3.1. Herein, $\mathbf{u}_J^\phi$ indicates the approximation computed by the traditional Galerkin scheme while $\mathbf{u}_J^\psi$ stands for the numerical solution of the wavelet Galerkin scheme. Note that for $J \geq 4$, that is $N_J \geq 12288$, we extrapolate the results of the single scale scheme since it is no more computable.

unknowns		scaling functions $\phi^{(1)}$		wavelets $\psi^{(1,3)}_{\text{tensor}}$	
J	N_J	$\|\mathbf{u} - \mathbf{u}_J^\phi\|_\infty$	contr.	$\|\mathbf{u} - \mathbf{u}_J^\psi\|_\infty$	contr.
1	192	1.7	—	9.7e-1	—
2	768	3.6e-1	4.6	2.3e-1	4.2
3	3072	6.5e-2	5.6	2.8e-2	8.5
4	12288	(1.6e-2)	(4.0)	8.4e-3	3.4
5	49152	(4.1e-3)	(4.0)	4.1e-3	2.0
6	196608	(1.0e-3)	(4.0)	7.2e-4	5.7

TABLE 3.1

The maximum norm of the absolute errors of the discrete potential.

In Table 3.1 we list the maximum norm of the absolute errors of $\mathbf{u}_J^\phi$ and $\mathbf{u}_J^\psi$. The latter one is tabulated only with respect to $\psi^{(1,3)}_{\text{optimized}}$ since the other wavelet bases yield nearly identical results. The columns titled by "contr." (contraction) contain the ratio of the absolute error obtained on the previous level divided by the present absolute error. The optimal order of convergence is quadratic which implies a contraction close to 4. As the results in Table 3.1 confirm, the precisions of the compressed wavelet Galerkin scheme is even higher than that of the single scale scheme.

Figure 3.2 is concerned with the the matrix compression and the computing times. The left plot visualizes the compression rates measured by the ratio (in %) of the number of nonzero matrix

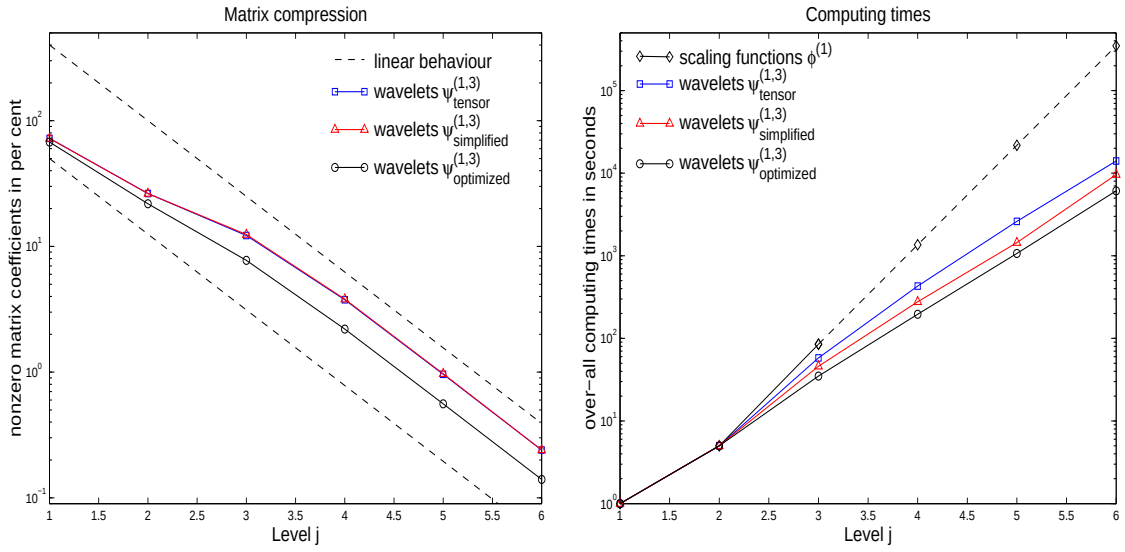

FIG. 3.2. *The compression rates and the computing times.*

coefficients and N_J^2. The best compression rates are achieved with respect to the wavelets $\psi^{(1,3)}_{\text{optimized}}$. which issues from their small supports. For 196608 unknows only 0.14% of the matrix coefficients are relevant. From the right plot one figures out the cpu-times required for computing and solving the linear system of equations resulting from the Galerkin scheme. The computing times of the single scale Galerkin scheme are extrapolated to the levels 4–6. The best performance is achieved by the wavelet Galerkin scheme based on $\psi^{(1,3)}_{\text{optimized}}$. For $N_J = 196608$ we obtain the speed-up factor 57 in comparison with the single scale scheme. We emphasize that the the wavelet Galerkin scheme based on the tensor product wavelets requires more than twice the cpu-time than that with respect to $\psi^{(1,3)}_{\text{optimized}}$. Consequently, these results justify our improvement of the wavelet bases.

3.2. Neumann Problem. For a given $g \in H^{-1/2}(\Gamma)$ with $\int_\Gamma g(\mathbf{x})d\sigma = 0$ we treat a Neumann problem on the domain Ω, that is, we seek $u \in H^1(\Omega)$ such that

$$\Delta u = 0 \text{ in } \Omega, \qquad \frac{\partial u}{\partial \mathbf{n}} = g \text{ on } \Gamma. \tag{3.5}$$

The considered domain Ω is described as the union of two spheres $B_1([0,0,\pm 2]^T)$ and one connecting cylinder with the radius 0.5, compare Figure 3.3. The boundary Γ is represented via 14 patches. Choosing the harmonical function

$$u(\mathbf{x}) = \frac{(\mathbf{a}, \mathbf{x}-\mathbf{b})}{\|\mathbf{x}-\mathbf{b}\|^3}, \quad \mathbf{a} = [1,2,4]^T, \quad \mathbf{b} = [1,0,0]^T.$$

and setting $g := \partial u|_\Gamma / \partial \mathbf{n}$, the Neumann problem has the solution u modulo a constant.

The *hypersingular operator* $\mathcal{W}$ is given by

$$\mathcal{W}\rho(\mathbf{x}) := -\frac{1}{4\pi}\frac{\partial}{\partial \mathbf{n}_\mathbf{x}} \int_\Gamma \frac{\partial}{\partial \mathbf{n}_\mathbf{y}} \frac{1}{\|\mathbf{x}-\mathbf{y}\|^2} \rho(\mathbf{y}) d\sigma_\mathbf{y}, \quad \mathbf{x} \in \Gamma,$$

and defines an operator of order +1. In order to solve problem (3.5) we seek the density ρ satisfying the Fredholm integral equation of the first kind

$$\mathcal{W}\rho = g \quad \text{on } \Gamma. \tag{3.6}$$

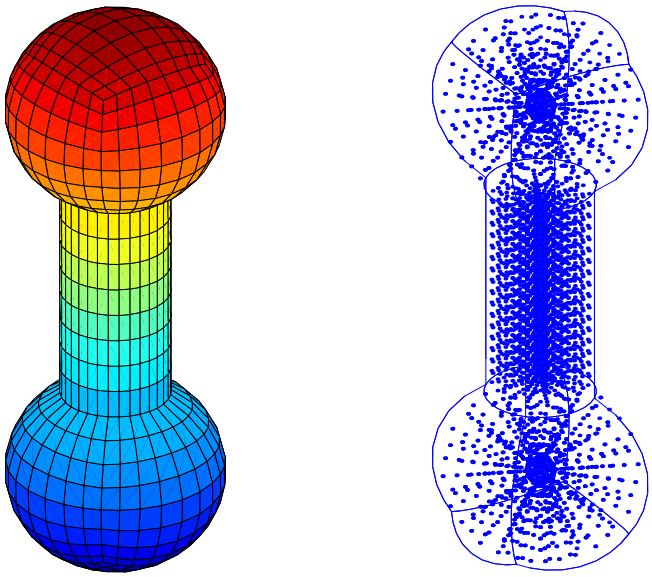

FIG. 3.3. *The mesh on the surface* Γ *and the evaluation points* $\mathbf{x}_i$ *of the potential.*

Since $\mathcal{W}$ is symmetric and positive semidefinite, cf. [20, 27], one restricts ρ by the constraint $\int_\Gamma \rho(\mathbf{x})d\sigma = 0$. We emphasize that the discretization of the hypersingular operator requires *globally continuous* piecewise linear wavelets. According to (1.14) piecewise linear wavelets have to provide two vanishing moments.

The density ρ given by the boundary integral equation (3.6) leads to the solution u of the Neumann problem by application of the double layer operator according to (3.3). The discrete counterparts are denoted as in (3.4), where the evaluation points $\mathbf{x}_i$ are specified in Figure 3.3.

First, we compare the errors of approximation with respect to the discrete potentials. The order of convergence is cubic (contraction 8) if the density is sufficiently smooth. The results in Table 3.2 suggest the we obtain this rate of convergence. But asymptotically one expects an order of convergence less than cubic due to concave angles between the patches. Finally we can see that the wavelet Galerkin scheme achieves the same accuracy as the traditional Galerkin scheme.

unknowns		scaling functions		wavelets $\psi^{(2,2)}_{\text{continuous}}$	
J	N_J	$\|\mathbf{u}_J - \mathbf{u}_J^\phi\|_\infty$	contr.	$\|\mathbf{u}_J - \mathbf{u}_J^\psi\|_\infty$	contr.
1	58	14	—	13	—
2	226	4.3	3.3	4.4	2.9
3	898	1.2	3.5	6.4e-1	6.9
4	3586	1.9e-1	6.3	4.4e-2	14
5	14338	(2.4e-2)	($\leq$8.0)	6.8e-3	6.5
6	57346	(3.0e-3)	($\leq$8.0)	3.2e-3	2.1

TABLE 3.2

The maximum norm of the absolute errors of the discrete potential.

The plots in Figure 3.4 visualize the compression rates and computing times. On the left hand side we plot the number of nonzero coefficients in percent. For 57346 unknowns the matrix compression yields only 1.32 % relevant matrix entries after the compression. On the right hand side one figures out the over-all computing times of the traditional discretization compared with those of the fast wavelet discretization. Note that we extrapolated the computing times of the traditional scheme to the levels 5 and 6. On level 6 the speed-up of the wavelet Galerkin scheme is about the factor 12 compared to the traditional scheme.

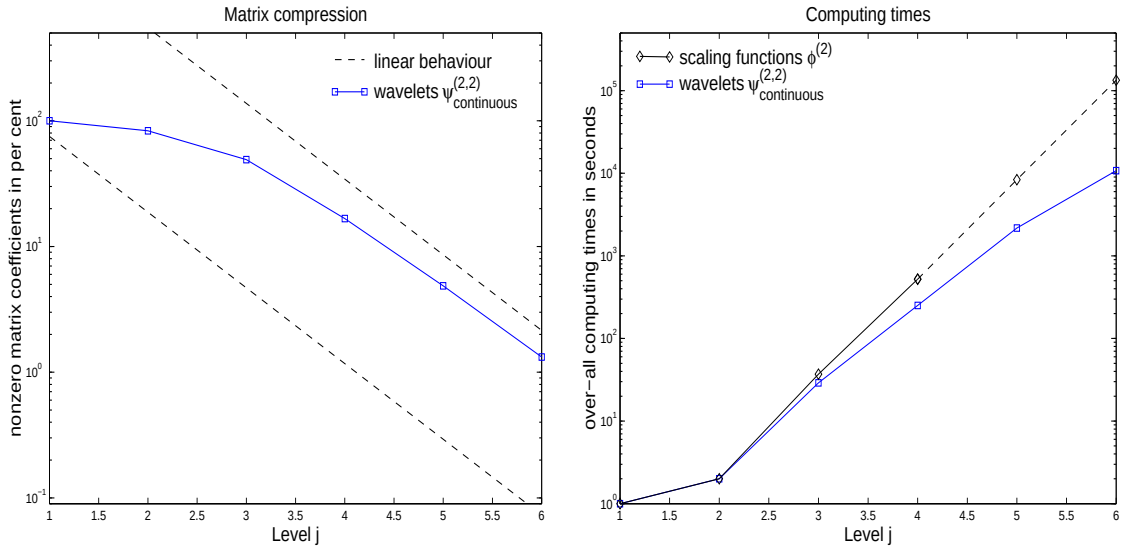

FIG. 3.4. *The compression rates and the computing times.*

REFERENCES

[1] G. Beylkin, R. Coifman, and V. Rokhlin. The fast wavelet transform and numerical algorithms. *Comm. Pure and Appl. Math.*, 44:141–183, 1991.

[2] C. Canuto, A. Tabacco, and K. Urban. The wavelet element method, part I: Construction and analysis. *Appl. Comput. Harm. Anal.*, 6:1–52, 1999.

[3] J. Carnicer, W. Dahmen, and J. Peña. Local decompositions of refinable spaces. *Appl. Comp. Harm. Anal.*, 3:127–153, 1996.

[4] A. Cohen, I. Daubechies, and J.-C. Feauveau. Biorthogonal bases of compactly supported wavelets. *Pure Appl. Math.*, 45:485–560, 1992.

[5] A. Cohen and R. Masson. Wavelet adaptive method for second order elliptic problems – boundary conditions and domain decomposition. *Numer. Math.*, 86:193–238, 2000.

[6] W. Dahmen. Wavelet and multiscale methods for operator equations. *Acta Numerica*, 6:55–228, 1997.

[7] W. Dahmen, H. Harbrecht and R. Schneider. Compression techniques for boundary integral equations – optimal complexity estimates. *Preprint SFB 393/02-06, TU Chemnitz*, 2002. submitted to SIAM J. Numer. Anal.

[8] W. Dahmen, B. Kleemann, S. Prößdorf, and R. Schneider. A multiscale method for the double layer potential equation on a polyhedron. In H.P. Dikshit and C.A. Micchelli, editors, *Advances in Computational Mathematics*, pages 15–57, World Scientific Publ., Singapore, 1994.

[9] W. Dahmen and A. Kunoth. Multilevel preconditioning. *Numer. Math.*, 63:315–344, 1992.

[10] W. Dahmen, A. Kunoth, and K. Urban. Biorthogonal spline-wavelets on the interval – stability and moment conditions. *Appl. Comp. Harm. Anal.*, 6:259–302, 1999.

[11] W. Dahmen, S. Prößdorf, and R. Schneider. Multiscale methods for pseudodifferential equations. In L.L. Schumaker and G. Webb, editors, *Wavelet Analysis and its Applications*, volume 3, pages 191–235, 1993.

[12] W. Dahmen, S. Prößdorf, and R. Schneider. Wavelet approximation methods for periodic pseudodifferential equations. Part II – Fast solution and matrix compression. *Advances in Computational Mathematics*, 1:259–335, 1993.

[13] W. Dahmen, S. Prößdorf, and R. Schneider. Wavelet approximation methods for periodic pseudodifferential equations. Part I – Convergence analysis. *Mathematische Zeitschrift*, 215:583–620, 1994.

[14] W. Dahmen, S. Prößdorf, and R. Schneider. Multiscale methods for pseudodifferential equations on smooth manifolds. In C.K. Chui, L. Montefusco, and L. Puccio, editors, *Proceedings of the International Conference on Wavelets: Theory, Algorithms, and Applications*, pages 385–424, 1995.

[15] W. Dahmen and R. Schneider. Wavelets on manifolds II: Application to boundary element methods and pseudodifferential equations, 1996. Manuscript.

[16] W. Dahmen and R. Schneider. Composite wavelet bases for operator equations. *Math. Comp.*, 68:1533–1567, 1999.

[17] W. Dahmen and R. Schneider. Wavelets on manifolds I. Construction and domain decomposition. *Math. Anal.*, 31:184–230, 1999.

[18] M. Duffy. Quadrature over a pyramid or cube of integrands with a singularity at the vertex. *SIAM J. Numer. Anal.*, 19:1260–1262, 1982.

[19] L. Greengard and V. Rokhlin. A fast algorithm for particle simulation. *J. Comput. Phys.*, 73:325–348, 1987.

[20] W. Hackbusch. *Integralgleichungen*. B.G. Teubner, Stuttgart, 1989.

[21] W. Hackbusch. A sparse matrix arithmetic based on $\mathcal{H}$-matrices. Part I: Introduction to $\mathcal{H}$-matrices. *Computing*, 64:89–108, 1999.

[22] W. Hackbusch and Z.P. Nowak. On the fast matrix multiplication in the boundary element method by panel clustering. *Numer. Math.*, 54:463–491, 1989.

[23] H. Harbrecht. Wavelet Galerkin schemes for the boundary element method in three dimensions. *PHD Thesis, Technische Universität Chemnitz, Germany*, 2001.

[24] H. Harbrecht, F. Paiva, C. Pérez, and R. Schneider. Biorthogonal wavelet approximation for the coupling of FEM-BEM. *Preprint SFB 393/99-32, TU Chemnitz*, 1999. to appear in Numer. Math.

[25] H. Harbrecht, F. Paiva, C. Pérez, and R. Schneider. Wavelet preconditioning for the coupling of FEM-BEM. *Preprint SFB 393/00-07, TU Chemnitz*, 2000. submitted to Numerical Linear Algebra with Applications.

[26] H. Harbrecht and R. Schneider. Wavelet Galerkin Schemes for 2D-BEM. In *Operator Theory: Advances and Applications*, volume 121. Birkhäuser, (2001).

[27] R. Kress. *Linear Integral Equations*. Springer-Verlag, Berlin-Heidelberg, 1989.

[28] T. von Petersdorff, R. Schneider, and C. Schwab. Multiwavelets for second kind integral equations. *SIAM J. Num. Anal.*, 34:2212–2227, 1997.

[29] T. von Petersdorff and C. Schwab. Fully discretized multiscale Galerkin BEM. In W. Dahmen, A. Kurdila, and P. Oswald, editors, *Multiscale wavelet methods for PDEs*, pages 287–346, Academic Press, San Diego, 1997.

[30] A. Rathsfeld. On a hierarchical three point basis of piecewise linear functions over smooth boundaries. In *Operator Theory: Advances and Applications*, volume 121. Birkhäuser, (2001).

[31] S. Sauter and C. Schwab. Quadrature for the *hp*-Galerkin BEM in $\mathbb{R}^3$. *Numer. Math.*, 78:211–258, 1997.

[32] R. Schneider. *Multiskalen- und Wavelet-Matrixkompression: Analysisbasierte Methoden zur Lösung großer vollbesetzter Gleichungssysteme.* B.G. Teubner, Stuttgart, 1998.

[33] W. Sweldens. The lifting scheme: A custom-design construction of biorthogonal wavelets. *Appl. Comput. Harmon. Anal.*, 3:186–200, 1996.

[34] E.E. Tyrtyshnikov. Mosaic sceleton approximation. *Calcolo*, 33:47–57, 1996.

[35] L. Villemoers. Wavelet analysis of refinement equations. *SIAM J. Math. Anal.*, 25:1433–1460, 1994.